

# 000 001 002 003 004 005 BRIDGING TEMPORAL AND SEMANTIC GAPS: PROMPT 006 LEARNING ON TEMPORAL INTERACTION GRAPHS 007 008 009

010 **Anonymous authors**  
011 Paper under double-blind review  
012  
013  
014  
015  
016  
017  
018  
019  
020  
021  
022  
023  
024  
025  
026

## ABSTRACT

027 Temporal Interaction Graphs (TIGs) are widely utilized to represent real-world sys-  
028 tems like e-commerce and social networks. While various TIG models have been  
029 proposed for representation learning, they face two critical gaps in their “pre-train,  
030 predict” training paradigm: a temporal gap limiting timely predictions and a se-  
031 mantic gap reducing adaptability to diverse downstream tasks. A potential solution  
032 is applying the “pre-train, prompt” paradigm, yet existing static graph prompting  
033 methods fail to address the time-sensitive dynamics of TIGs and have a deficiency  
034 in expressive power. To tackle these issues, we propose **Temporal Interaction**  
035 **Graph Prompting (TIGPrompt)**, a versatile framework that bridges the tempo-  
036 ral and semantic gaps by integrating with existing TIG models. Specifically, we  
037 propose a “pre-train, prompt” training paradigm for TIGs, with a temporal prompt  
038 generator to offer temporally-aware prompts for different tasks. To cater to varying  
039 computational resource demands, we propose an extended “pre-train, prompt-based  
040 fine-tune” paradigm, offering greater flexibility. Through extensive experiments  
041 involving multiple benchmarks, representative TIG models, and downstream tasks,  
042 our TIGPrompt demonstrates the SOTA performance and remarkable efficiency  
043 advantages. The codes are available at an Anonymous Repository.  
044

## 1 INTRODUCTION

045 In real-world scenarios, interaction data is often accompanied by temporal information, i.e., times-  
046 tamps, necessitating its modeling as Temporal Interaction Graphs (TIGs) (Dai et al., 2016; Zhang  
047 et al., 2017). In this context, static graphs can hardly model such TIGs since they lack the necessary  
048 expressiveness to capture temporal dependencies. Specifically, in TIGs, objects are depicted as  
049 nodes, while timestamped interactions between these objects are represented as edges. Consequently,  
050 significant research efforts have been dedicated to TIG representation learning models (TIG models)  
051 (Trivedi et al., 2019; Xu et al., 2020; Rossi et al., 2020; Zhang et al., 2023c). These works aim to  
052 capture the dynamic nature of TIGs and learn temporal node representations, which can be applied to  
053 various downstream tasks (Kumar et al., 2019; Rossi et al., 2020; Zhang et al., 2023c).

054 **The “pre-train, predict” paradigm of existing TIG models.** Recently, researchers have tried  
055 to explore the design of TIG models, leading to various effective TIG model structures (Zhang  
056 et al., 2023c;b;a). For example, TGN (Rossi et al., 2020) employs a memory module to store  
057 historical information of nodes and a message module to store current node embeddings, each with  
058 an associated update function that updates the memory and node representations. Although powerful,  
059 as illustrated in Fig. 2 (a), we observe that nearly all of these models adopt a “*pre-train, predict*”  
060 learning framework, where a TIG model is pre-trained on a specific task (e.g., link prediction) and  
061 its learned knowledge is then transferred to various downstream tasks by tuning a corresponding  
062 predictor (e.g., MLP (Bishop & Nasrabadi, 2006)).

063 **Limitations of the “pre-train, predict” paradigm.** In this paper, we analyze the prevailing “pre-  
064 train–predict” paradigm in TIG models and identify two critical limitations: the **temporal gap** and  
065 the **semantic gap**. First, as temporal interactions evolve, pre-trained models quickly become outdated,  
066 leading to degraded performance on distant-future data (i.e., the **temporal gap**) (Zhou et al., 2022;  
067 Chen et al., 2023b). As shown in Fig. 1 (a), our preliminary experiments simulate this scenario and  
068 reveal a clear performance disparity between temporally proximal and temporally distant inference  
069 data, providing evidence of the existence of the temporal gap. However, mitigating this gap under  
070

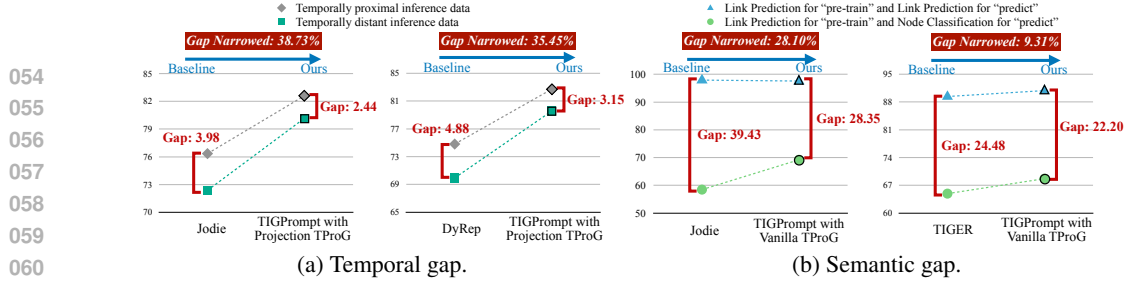


Figure 1: Empirical analysis of the temporal gap and semantic gap on real-world TIG data. Our proposed TIG-Prompt can effectively narrow these two gaps for better TIG representation learning. For more implementation details, please refer to Appendix A.

the “pre-train, predict” paradigm typically requires exhaustive re-training to incorporate new data recursively into model updating, resulting in a significant consumption of computational resources (Devlin et al., 2018). Second, misalignment between pretext tasks and downstream objectives significantly limits transferability across tasks (i.e., the **semantic gap**). For instance, while most TIG models are pre-trained on edge-level prediction, downstream tasks may involve node-level objectives, which can even cause negative transfer (Sun et al., 2023). Fig. 1 (b) further validates the existence of this semantic gap. Such misalignment reduces the adaptability of TIG models, thereby constraining their effectiveness in handling various downstream tasks. The detailed definitions, illustrative examples, and quantification of the two gaps are provided in the Appendix A.

**Prompt learning paradigm on static graphs.** The aforementioned two gaps caused by the “pre-train, predict” paradigm call for a more flexible training paradigm for TIG models. Graph prompt learning offers such a potential solution by enabling efficient adaptation of pre-trained models through the design and training of lightweight prompts, while keeping the backbone model unchanged (Liu et al., 2023b; Fang et al., 2023). As demonstrated in static graph settings, prompt learning can not only reduce the cost of adapting models to evolving data compared with full re-training (Liu et al., 2023a), but also explicitly incorporate task-specific knowledge through prompt vectors (Sun et al., 2023), thereby providing greater flexibility than traditional learning frameworks.

**Limitations of existing graph prompt learning paradigm.** Existing studies on prompt learning for graphs have predominantly focused on static settings (Sun et al., 2022), providing limited insights into the more complex scenario of TIGs. Most of these methods overlook the temporal nature of TIGs, failing to incorporate temporal information into prompts to capture their evolving characteristics (Dai et al., 2016). In addition, current approaches typically employ over-simplified prompt vectors shared across all nodes (Liu et al., 2023b). While such designs may suffice for static graphs, they are inadequate for TIGs, where node representations evolve continuously and demand personalized updates over time. These limitations give rise to two technical challenges that hinder the direct application of traditional static graph prompt learning to TIGs. The **first challenge** is how to learn expressive prompts with the minimal cost to overcome the temporal gap caused by emerging data. The **second challenge** is how to design flexible and temporal-aware prompts that can support various TIG models and break down the semantic gap within diverse downstream application scenarios.

**Present work.** In this paper, we propose a new training architecture for TIG models, namely Temporal Interaction Graph Prompting (**TIGPrompt**), as shown in Fig. 2 (b). TIGPrompt instantiates a “pre-train, prompt” paradigm through a **Temporal Prompt Generator (TProG)**, which intelligently generates personalized temporal prompts for each node. By explicitly incorporating temporal information, the prompts adapt to timestamp-specific variability, thereby bridging the temporal gap and overcoming the limitations of static graph prompting methods. Furthermore, to mitigate the semantic gap between pretext and downstream tasks, the TProG is jointly tuned with the specific downstream task, facilitating adaptability to concrete down-

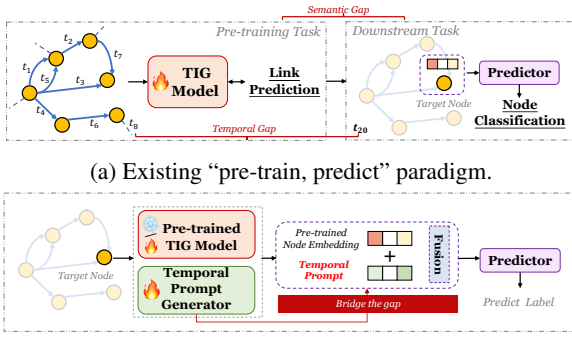


Figure 2: (a): The “pre-train, predict” paradigm adopted by existing TIG models, which exhibits both temporal and semantic gaps when applied on the downstream task. (b): Our introduced prompting mechanism, with an innovative TProG, designed to mitigate both gaps.

108 stream scenarios. Notably, TIGPrompt is lightweight, as it involves only tuning the TIGPrompt while  
 109 keeping the TIG model frozen. It is also tolerant to weak supervision, requiring only a small portion of  
 110 data for pre-training and prompt tuning. Furthermore, we extend the “pre-train, prompt” paradigm to  
 111 cater to varying computational resource demands by introducing a “*pre-train, prompt-based fine-tune*”  
 112 solution. We summarize our contributions as follows:

- 113 • We identify two critical gaps in the prevailing TIG training paradigm and study the prompting  
 114 mechanism on TIG models. This is the first attempt that explores prompting on TIGs.
- 115 • We propose a “pre-train, prompt” paradigm specifically tailored for TIGs, bridging both the  
 116 temporal and semantic gaps in the traditional training process. Meanwhile, our framework  
 117 is compatible with various prompt generators and enables dynamic, personalized prompting.
- 118 • To enhance the flexibility and accommodate diverse computational resources, we extend  
 119 the paradigm to a “pre-train, prompt-based fine-tune” solution. Both paradigms can be  
 120 seamlessly integrated with existing TIG models.
- 121 • Extensive experiments on four datasets with seven representative TIG models across two  
 122 downstream tasks demonstrate that our framework achieves SOTA performance with re-  
 123 markable efficiency.

## 124 2 PRELIMINARIES

125 **126 Definition of TIG.** Given a node set  $\mathcal{V} = \{1, \dots, |\mathcal{V}|\}$  and a sequence of time-stamped edges  
 127  $\mathcal{E} = \{(u, v, t_{uv}) \mid u, v \in \mathcal{V}, t_{uv} > 0\}$ , where each edge  $(u, v, t_{uv})$  denotes an interaction between  
 128 nodes  $u$  and  $v$  at time  $t_{uv}$ , a TIG is defined as  $\mathcal{G} = (\mathcal{V}, \mathcal{E})$ . Each interaction may be associated with a  
 129 feature vector  $\mathbf{e}_{uv}(t)$ , which encodes event-specific attributes such as interaction type or contextual  
 130 information. For any interaction  $(u, v, t_{uv}) \in \mathcal{E}$ , the model has access only to historical events  
 131 occurring before time  $t_{uv}$ , i.e.,  $(i, j, \tau) \in \mathcal{E} \mid \tau < t_{uv}$ .

132 **133 TIG Models.** Given an interaction event  $(u, v, t_{uv}) \in \mathcal{E}$  and its corresponding historical inter-  
 134 action records  $(u, v, \tau) \in \mathcal{E} \mid \tau < t_{uv}$ , TIG models aim to learn a mapping  $f_{\Theta} : (u, v, t_{uv}) \mapsto$   
 135  $\mathbf{z}_u(t_{uv}), \mathbf{z}_v(t_{uv})$ , where  $\mathbf{z}_u(t_{uv}), \mathbf{z}_v(t_{uv}) \in \mathbb{R}^d$  represent the dynamic embeddings of nodes  $u$  and  
 136  $v$  at time  $t_{uv}$ , and  $d$  denotes the dimensionality of the embedding space. At the whole-graph level,  
 137 the model’s output can be equivalently expressed as  $\mathbf{Z} = f_{\Theta}(\mathcal{V}, \mathcal{E})$ , which yields the time-evolving  
 138 representations for all nodes in the graph.

139 **140 Downstream Tasks.** After optimizing the backbone TIG model, the node representations produced  
 141 by an arbitrary TIG encoder  $f_{\Theta}(\cdot)$  can be retrieved for downstream tasks, formulated as  $\hat{\mathbf{Y}} = p_{\Phi}(\mathbf{Z})$ ,  
 142 where  $p_{\Phi}(\cdot)$  denotes the task-specific projection head (i.e. predictor).

143 For the link prediction task, the model estimates whether an interaction between two nodes will occur  
 144 at a future time, typically expressed as  $p_{\Phi}(\mathbf{z}_u(t), \mathbf{z}_v(t)) \rightarrow \hat{y}_{uv}(t)$ . This objective also serves as  
 145 the pretext task adopted by most TIG models. Since the supervision signal (future interactions) is  
 146 inherently available in the TIG, this training paradigm is self-supervised.

147 For the node classification task, the model predicts node-level labels (e.g., user categories or item  
 148 types) using the learned dynamic node embeddings:  $p_{\Phi}(\mathbf{z}_u(t)) \rightarrow \hat{y}_u$ . Here,  $p_{\Phi}$  is an additional  
 149 trainable projection head that is optimized separately from the TIG encoder, and its training requires  
 150 labeled node instances. As a result, node classification introduces an explicit supervised phase on top  
 151 of the self-supervised TIG pre-training, where link prediction serves as the pretext task.

## 152 3 PROPOSED METHOD

153 In this section, we elaborate on the detailed designs within the TIGPrompt framework. We first  
 154 provide an overview of the “pre-train, prompt” paradigm. Then, we show the implementation and  
 155 optimization of our Temporal Prompt Generator (TProG) component, which enables the adaptability  
 156 of pre-trained models across diverse downstream tasks. Finally, we extend this paradigm to the  
 157 “pre-train, prompt-based fine-tune” mode, specifically devised to accommodate varying computing  
 158 resource constraints. An overview of our method is illustrated in Fig. 3.

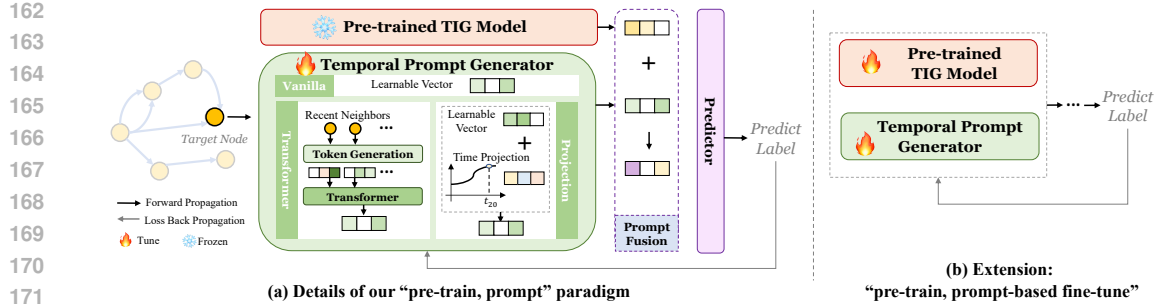


Figure 3: Overview of TIGPrompt: (a) During the prompt tuning stage, the node embedding, calculated by the pre-trained TIG model, is combined with the personalized prompt embedding for downstream tasks. The TProG is optimized during this stage. (b) The key distinction between the two modes lies in whether the parameters of the TIG model are tuned.

### 3.1 “PRE-TRAIN, PROMPT” PARADIGM OVERVIEW

Existing TIG models such as JODIE (Kumar et al., 2019), DyRep (Trivedi et al., 2019), TGN (Rossi et al., 2020), and TIGER (Zhang et al., 2023c) primarily employ link prediction as the pre-training objective, with differences in their concrete model implementation. For instance, TGN (Rossi et al., 2020) introduces a memory-based approach and integrates previous works into a cohesive framework, while TIGER (Zhang et al., 2023c) puts forward a model that incorporates a dual-memory module for effective information aggregation. Once a TIG model is well-trained, node embeddings can be retrieved for task-specific predictions, such as node classification. The predictions are made as:  $\hat{Y} = p_\Phi(\mathbf{Z})$ , where  $\mathbf{Z} = f_\Theta(\mathcal{V}, \mathcal{E})$ . Here,  $p_\Phi(\cdot)$  denotes the projection head of the downstream task,  $\mathbf{Z}$  denotes the learned node representations obtained from an arbitrary TIG model  $f_\Theta(\cdot)$ , which takes a TIG,  $G(\mathcal{V}, \mathcal{E})$  as input. However, it is important to note that directly utilizing pre-trained node embeddings for downstream tasks is unfeasible as it overlooks two critical gaps: the temporal gap (i.e., the evolving nature of TIGs may render pre-trained node embeddings less expressiveness to the timely TIG data), and the semantic gap (i.e., the distinctions between link-level pretext task and node-level downstream task).

To bridge these gaps and enable the adaptability of a pre-trained TIG model across various scenarios, we propose to utilize personalized and temporal-aware *prompt* for each node. Combined with pre-trained node embeddings, these prompts can carry task-specific semantics to get adapted to different downstream tasks as:

$$\hat{Y} = p_\Phi(\tilde{\mathbf{Z}}), \quad \tilde{\mathbf{Z}} = f_\rho(\mathbf{Z}, \mathbf{P}), \quad (1)$$

where  $\mathbf{P}$  denotes the prompt matrix produced by the TProG,  $f_\rho(\cdot)$  represents the fusion function, and  $\tilde{\mathbf{Z}}$  denotes the final prompted node representations. The prompt generator is tuned with task-specific supervision, enabling the final synthesized node representations contain task-specific and temporal-aware knowledge. Notably, during this process, the pre-trained TIG model  $f_\Theta(\cdot)$  remains frozen, making TIGPrompt lightweight to get adapted to concrete downstream scenarios. Then, we move to the description of how these prompts are generated and tuned.

### 3.2 TPROG: TEMPORAL PROMPT GENERATOR

In this subsection, we provide a detailed explanation of our implementation of TProG, which produces a prompt matrix  $\mathbf{P} \in \mathbb{R}^{|\mathcal{V}| \times d}$ . We initially introduce a *Vanilla* TProG, where a learnable vector is assigned to each node, enabling personalized prompts tailored for specific downstream scenarios. Note that *Vanilla* TProG can be considered an intermediate bridge between static and temporal interaction graph prompt learning, since it generates personalized prompts but does not inject temporal information. To enhance the temporal awareness of produced prompts, we extend the TProG by introducing two additional approaches: the *Transformer* TProG and the *Projection* TProG.

**Vanilla TProG.** We first introduce the simplest version of TProG, which aims to provide personalized expressiveness for each node. In this approach, the prompt for node  $v \in \mathcal{V}$  is implemented as a learnable vector  $\mathbf{p}_v \in \mathbb{R}^d$ , which is initialized as zero vector. Current methods normally utilize the

link prediction task as the pretext task. In downstream tasks such as node classification, a projection head—commonly an MLP—is used to classify node embeddings derived from the pre-trained model. We enhance these node embeddings with learnable prompt vectors, i.e., Vanilla TProG, which are concurrently optimized with the downstream task’s projection head. This strategy effectively embeds task-specific knowledge into the prompt vectors during the prompt tuning phase. This implementation bears a resemblance to traditional prompting techniques utilized in static graphs (Fang et al., 2023; Liu et al., 2023b), and serves as a conceptual bridge between traditional graph prompting and TIG prompt methods. Despite its simplicity, this method offers an intuitive design, easy implementation, and low parameterization, requiring only  $\mathcal{O}(|\mathcal{V}|)$  parameters, scaling linearly with the size of the temporal interaction graph.

**Transformer TProG.** To generate temporal-aware prompt, we consider encoding the most relevant temporal information for each node. For a target node  $v$ , its most recent interactions provide valuable insights into its temporal information, which can be leveraged to generate the temporal prompt  $\mathbf{p}_v$ .

Therefore, at any timestamp  $t$ , we first retrieve the node’s most recent neighbor set  $\mathcal{N}_v^t = \{u|u \in \mathcal{V}, (u, v, t_{uv}) \in \mathcal{E} \text{ and } t_{uv} \leq t\}$ . To avoid an excessively large neighbor set, we impose a restriction on the size of  $\mathcal{N}_v^t$ , returning only the most recent  $K$  interactions. Then, for each neighboring node  $u \in \mathcal{N}_v^t$ , we first create a temporal neighbor token as:  $\mathbf{t}_u = \mathbf{z}_v \parallel \mathbf{z}_u \parallel \mathbf{pos}_u \parallel \mathbf{e}_{uv} \parallel f_\omega(t - t_{uv})$ , where  $\mathbf{z}_u, \mathbf{z}_v$  are pre-trained node embeddings,  $\mathbf{pos}_u$  corresponds to the position index of node  $u$  within the neighbor set,  $\mathbf{e}_{uv}$  denotes the edge feature of historical interaction  $(u, v, t_{uv})$ ,  $\parallel$  denotes the concatenation operation, and  $f_\omega(\cdot)$  denotes a time encoding function (we apply the same time encoding method used in (Xu et al., 2020; Rossi et al., 2020; Zhang et al., 2023c)). In this way, the neighboring token  $\mathbf{t}_u$  incorporates both interactive and temporal knowledge, and we further leverage a Transformer (Vaswani et al., 2017) to encode those temporal neighboring tokens to generate temporal prompt  $\mathbf{p}_v$  as:

$$\mathbf{p}_v = \text{Transformer}(\{\mathbf{t}_u|u \in \mathcal{N}_v^t\}). \quad (2)$$

This approach ensures that the generated prompt  $\mathbf{p}_v$  captures expressive temporal and recent interactive knowledge, promising to enhance downstream predictions. The implementation of Transformer TProG is extremely lightweight, as the number of tunable parameters within this component is  $\mathcal{O}(d)$ , scaling linearly with the embedding dimension.

**Projection TProG.** In addition to encoding recent neighboring information, we can also generate a temporal-aware prompt by integrating personalized vectors and time encoding. Recall that in the Vanilla TProG, we introduce a learnable vector  $\mathbf{p}_v^{\text{Personal}} \in \mathbb{R}^d$  for each node to represent the prompt. To incorporate the temporal knowledge, we fuse this personalized vector with time encoding. Specifically, at timestamp  $t$ , the temporal information can be encoded as  $\mathbf{p}_v^{\text{Temporal}} = f_\omega(t - t_{v'})$ , where  $t_{v'}$  represents the most recent interaction timestamp of node  $v$ , and  $f_\omega(\cdot)$  is a time encoding function. Finally, the temporal prompt  $\mathbf{p}_v$  is generated via integrating both sides of information as:

$$\mathbf{p}_v = \text{MLP}(\mathbf{p}_v^{\text{Personal}} \parallel \mathbf{p}_v^{\text{Temporal}}), \quad (3)$$

where  $\text{MLP}(\cdot)$  (Bishop & Nasrabadi, 2006) is introduced to combine two types of information. The Projection TProG can be seen as a middle ground between the Vanilla TProG and the Transformer TProG, as it utilizes a learnable prompt vector to represent interactive information and a temporal vector to mimic the temporal evolution. Like the Vanilla TProG, the number of tunable parameters required for the Projection TProG is  $\mathcal{O}(|\mathcal{V}|)$ , scaling linearly with the size of the graph.

### 3.3 PROMPT TUNING AND INFERENCE

Recall in Equ. 1, a fusion function is introduced to combine pre-trained node embeddings  $\mathbf{Z}$  and prompt matrix  $\mathbf{P}$  to yield prompted node representations. Specifically, we implement  $f_\rho(\cdot)$  via a MLP parameterized by  $\rho$  as:

$$\tilde{\mathbf{Z}} = f_\rho(\mathbf{Z}, \mathbf{P}) = \text{MLP}_\rho(\mathbf{Z} \parallel \mathbf{P}), \quad (4)$$

where  $\tilde{\mathbf{Z}}$  can be regarded as prompted embeddings, incorporating temporal knowledge to adapt to specific downstream tasks.

Take the downstream link prediction task as an example, suppose a TIG has edge set  $\mathcal{E}$ , which can be split into three disjoint sets as  $\mathcal{E} = \mathcal{E}^{\text{pre-train}} \cup \mathcal{E}^{\text{prompt}} \cup \mathcal{E}^{\text{val/test}}$ . Here,  $\mathcal{E}^{\text{pre-train}}$  denotes the

270 set of edges used for pre-training the TIG model  $f_\Theta(\cdot)$ ,  $\mathcal{E}^{\text{prompt}}$  represents the set used to tune  
 271 the prompt generator, and  $\mathcal{E}^{\text{val/test}}$  denotes the edges for validation or testing. Specifically, given  
 272  $\mathcal{E}^{\text{prompt}}$ , the TProG is optimized using predictions and ground-truth labels:  $\mathcal{L}_{\text{prompt-tune}}(\Phi, \rho, \mathbf{P}) =$   
 273 Cross-Entropy( $p_\Phi(f_\rho(\mathbf{Z}, \mathbf{P}))$ ,  $\mathbf{Y}^{\text{prompt}}$ ), where  $\mathbf{Y}^{\text{prompt}}$  denotes the ground-truth labels provided by  
 274  $\mathcal{E}^{\text{prompt}}$ ,  $p_\Phi(\cdot)$  denotes the projection head of the link prediction task. Notably, during the prompt  
 275 tuning stage, the TIG model remains frozen, avoiding exhaustive re-training processes. The tuning  
 276 data only constitutes a small portion, meaning that even a small number of samples can help  
 277 improve the adaptation of the pre-trained TIG model to downstream predictions. Similarly, the  
 278 downstream node classification task can provide a small number of samples to tune TProG and  
 279 generate meaningful  $\mathbf{P}$ . Once TProG is well-tuned, downstream predictions can be made as  $\hat{\mathbf{Y}} =$   
 280  $p_\Phi(f_\rho(\mathbf{Z}, \mathbf{P}))$ . By leveraging task-specific supervision to tune TProG, the prompts can incorporate  
 281 task-specific semantics. This tuning process helps bridge both semantic and temporal gaps, resulting  
 282 in improved downstream predictions.

283 **Extension: “Pre-train, Prompt-based Fine-tune” Paradigm.** To accommodate to diverse computational  
 284 resource requirements, we extend the proposed “pre-train, prompt” paradigm to the “pre-train,  
 285 prompt-based fine-tune” paradigm. The main difference between these two modes lies in whether  
 286 the parameters of TIG model  $f_\Theta(\cdot)$  is tuned during the prompt tuning stage. Therefore, for this  
 287 paradigm, given prompt samples, both the prompts and the TIG model are optimized concurrently  
 288 as:  $\mathcal{L}_{\text{fine-tune}}(\Phi, \rho, \mathbf{P}, \Theta) = \text{Cross-Entropy}(p_\Phi(f_{\rho, \Theta}(\mathbf{Z}, \mathbf{P})), \mathbf{Y}^{\text{prompt}})$ . By jointly optimizing the TIG  
 289 model and the prompts, these two components reinforce each other, leading to improved adaptability  
 290 in various scenarios.

### 291 3.4 CONNECTION TO EXISTING GRAPH PROMPTING APPROACHES

293 Various prompting methods have been developed for static graphs (Please refer to Appendix B Related  
 294 Work for more details). Most of these methods are specifically designed for a range of downstream  
 295 tasks unique to static graph contexts. Among these methods, GraphPrompt (Liu et al., 2023b) and  
 296 GPF (Fang et al., 2023) stand out as representatives and amenable to adaptation for the TIG model.  
 297 GraphPrompt (Liu et al., 2023b) utilizes a prompt vector on the outputted embeddings of GNN  
 298 models, whereas GPF (Fang et al., 2023) employs a similar prompt vector on the input data features.  
 299 Therefore, in Sec. 4.5 we transfer these ideas to the TIG model and conduct experiments to see the  
 300 comparable performance with our temporal graph prompting approach.

## 301 4 EXPERIMENTS

### 304 4.1 DATASETS AND BASELINES

306 We apply the proposed TIGPrompt on four public datasets, Wikipedia, Reddit, MOOC and LastFM  
 307 (Kumar et al., 2019). Detailed statistics of these datasets are presented in Appendix C (Tab. 5). Only  
 308 Wikipedia, Reddit and MOOC are with dynamic labels indicating state changes of users. For datasets  
 309 missing node or edge features, we adopt the approach used in prior works (Rossi et al., 2020; Zhang  
 310 et al., 2023c), representing them with zero vectors.

311 For baseline comparisons, we select representative TGN-based methods<sup>1</sup>, including Jodie (Kumar  
 312 et al., 2019), DyRep (Trivedi et al., 2019), TGN (Rossi et al., 2020) and TIGE (Zhang et al., 2023c).  
 313 Additionally, we include TIGER-T (Zhang et al., 2023c) as a baseline, considering it is a variant  
 314 of TIGE and potentially offers improved performance over the TIGE model. We also compare  
 315 our method with GraphMixer (Cong et al., 2023) and DyGFormer (Yu et al., 2023), which employ  
 316 different model architectures, with a detailed discussion provided in Appendix E.2.

### 317 4.2 EXPERIMENTAL SETTINGS

319 Our implementation and hyper-parameter settings are consistent with those in previous works (Rossi  
 320 et al., 2020; Zhang et al., 2023c). More information is discussed in Appendix J. Typically, the chosen  
 321 baseline models split interaction edges chronologically into 70% for training, 15% for validation, and  
 322 15% for testing. However, as discussed in Sec. 3, our aim is to demonstrate our method’s adeptness

323 <sup>1</sup>These methods can be integrated into a unified framework based on TGN (Rossi et al., 2020).

324  
 325  
 326  
 327  
 328  
 Table 1: Under the “pre-train, prompt” paradigm, results for the link prediction task — encompassing  
 both transductive and inductive settings — are presented using Average Precision (%). For the  
 dynamic node classification task, results are measured in terms of AUROC (%). The best performance  
 is highlighted in **bold**.

Transductive Link Prediction												Inductive Link Prediction			Node Classification								
TProG		Wiki		Reddit		MOOC		LastFM		Wiki		Reddit		MOOC		LastFM		Wiki		Reddit		MOOC	
331 332 333 334 335 336 337 338 339 340 341 342 343 344 345 346 347 348 349	331 332 333 334 335 336 337 338 339 340 341 342 343 344 345 346 347 348 349	331 332 333 334 335 336 337 338 339 340 341 342 343 344 345 346 347 348 349	Baseline	94.62 $\pm$ 0.5	97.11 $\pm$ 0.3	76.50 $\pm$ 1.8	68.77 $\pm$ 3.0	93.11 $\pm$ 0.4	94.36 $\pm$ 1.1	77.83 $\pm$ 2.1	82.55 $\pm$ 1.9	86.27 $\pm$ 2.2	58.48 $\pm$ 2.6	65.39 $\pm$ 1.1	69.22 $\pm$ 0.4	69.21 $\pm$ 0.4	60.77 $\pm$ 2.2	63.80 $\pm$ 2.2	70.67 $\pm$ 1.1	68.26 $\pm$ 0.9	76.45 $\pm$ 0.6		
			Vanilla	94.10 $\pm$ 0.4	97.65 $\pm$ 0.0	74.47 $\pm$ 0.9	74.15 $\pm$ 1.0	91.43 $\pm$ 0.3	93.07 $\pm$ 0.4	72.23 $\pm$ 1.4	79.42 $\pm$ 1.1	86.79 $\pm$ 2.1	69.22 $\pm$ 0.4	69.21 $\pm$ 0.4	60.77 $\pm$ 2.2	63.80 $\pm$ 2.2	70.67 $\pm$ 1.1	68.26 $\pm$ 0.9	76.45 $\pm$ 0.6				
			Transformer	96.50 $\pm$ 0.1	98.28 $\pm$ 0.0	82.90 $\pm$ 1.1	77.98 $\pm$ 2.1	95.08 $\pm$ 0.2	95.68 $\pm$ 0.1	79.81 $\pm$ 1.2	85.72 $\pm$ 0.9	80.91 $\pm$ 1.6	63.80 $\pm$ 2.2	70.67 $\pm$ 1.1	68.26 $\pm$ 0.9	76.45 $\pm$ 0.6	70.80 $\pm$ 0.9	76.45 $\pm$ 0.6					
			Projection	96.44 $\pm$ 0.3	98.99 $\pm$ 0.0	82.47 $\pm$ 0.9	89.39 $\pm$ 0.7	94.75 $\pm$ 0.5	97.43 $\pm$ 0.1	79.89 $\pm$ 1.2	92.72 $\pm$ 0.4	87.08 $\pm$ 1.1	68.26 $\pm$ 0.9	76.45 $\pm$ 0.6	70.80 $\pm$ 0.9	76.45 $\pm$ 0.6	70.80 $\pm$ 0.9	76.45 $\pm$ 0.6					
331 332 333 334 335 336 337 338 339 340 341 342 343 344 345 346 347 348 349	331 332 333 334 335 336 337 338 339 340 341 342 343 344 345 346 347 348 349	331 332 333 334 335 336 337 338 339 340 341 342 343 344 345 346 347 348 349	Baseline	94.59 $\pm$ 0.2	97.98 $\pm$ 0.1	75.37 $\pm$ 1.7	68.77 $\pm$ 2.1	92.05 $\pm$ 0.3	95.68 $\pm$ 0.2	78.55 $\pm$ 1.1	81.33 $\pm$ 2.1	85.11 $\pm$ 1.4	62.77 $\pm$ 2.1	66.68 $\pm$ 3.4	68.38 $\pm$ 0.9	65.67 $\pm$ 2.4	65.67 $\pm$ 2.4	60.87 $\pm$ 3.8	58.20 $\pm$ 2.3	70.80 $\pm$ 0.9	64.50 $\pm$ 1.5	76.06 $\pm$ 0.9	
			Vanilla	89.64 $\pm$ 1.0	97.63 $\pm$ 0.0	71.57 $\pm$ 2.7	72.62 $\pm$ 1.1	85.45 $\pm$ 1.2	92.92 $\pm$ 0.3	71.34 $\pm$ 0.5	77.48 $\pm$ 1.7	84.88 $\pm$ 1.4	65.67 $\pm$ 2.4	65.67 $\pm$ 2.4	60.87 $\pm$ 3.8	58.20 $\pm$ 2.3	70.80 $\pm$ 0.9	64.50 $\pm$ 1.5	76.06 $\pm$ 0.9				
			Transformer	94.51 $\pm$ 0.4	98.27 $\pm$ 0.0	80.59 $\pm$ 1.9	76.89 $\pm$ 1.6	92.44 $\pm$ 0.4	95.73 $\pm$ 0.1	78.89 $\pm$ 0.2	84.81 $\pm$ 3.0	60.87 $\pm$ 3.8	64.89 $\pm$ 1.1	71.13 $\pm$ 1.4	71.13 $\pm$ 1.4	60.87 $\pm$ 3.8	58.20 $\pm$ 2.3	70.80 $\pm$ 0.9	64.50 $\pm$ 1.5	76.06 $\pm$ 0.9			
			Projection	96.87 $\pm$ 0.2	99.06 $\pm$ 0.0	79.76 $\pm$ 1.9	89.04 $\pm$ 0.6	95.37 $\pm$ 0.3	97.48 $\pm$ 0.0	78.56 $\pm$ 0.7	92.58 $\pm$ 0.4	85.25 $\pm$ 1.3	64.50 $\pm$ 1.5	76.06 $\pm$ 0.9	76.06 $\pm$ 0.9	64.50 $\pm$ 1.5	76.06 $\pm$ 0.9	76.06 $\pm$ 0.9					
331 332 333 334 335 336 337 338 339 340 341 342 343 344 345 346 347 348 349	331 332 333 334 335 336 337 338 339 340 341 342 343 344 345 346 347 348 349	331 332 333 334 335 336 337 338 339 340 341 342 343 344 345 346 347 348 349	Baseline	98.46 $\pm$ 0.1	98.70 $\pm$ 0.1	85.88 $\pm$ 3.0	71.76 $\pm$ 5.3	97.81 $\pm$ 0.1	97.55 $\pm$ 0.1	85.55 $\pm$ 2.9	80.42 $\pm$ 4.9	84.93 $\pm$ 1.1	65.99 $\pm$ 3.8	69.80 $\pm$ 1.8	66.13 $\pm$ 1.3	70.16 $\pm$ 1.1	70.16 $\pm$ 1.1	68.39 $\pm$ 1.0	66.13 $\pm$ 1.3	70.16 $\pm$ 1.1	66.07 $\pm$ 1.5	73.44 $\pm$ 1.4	
			Vanilla	96.40 $\pm$ 0.2	98.36 $\pm$ 0.0	86.71 $\pm$ 1.0	79.67 $\pm$ 1.7	95.02 $\pm$ 0.2	95.54 $\pm$ 0.2	81.99 $\pm$ 1.2	83.76 $\pm$ 1.3	85.79 $\pm$ 1.1	66.13 $\pm$ 1.3	70.16 $\pm$ 1.1	70.16 $\pm$ 1.1	68.39 $\pm$ 1.0	66.13 $\pm$ 1.3	70.16 $\pm$ 1.1	66.07 $\pm$ 1.5	73.44 $\pm$ 1.4			
			Transformer	97.36 $\pm$ 0.2	98.67 $\pm$ 0.0	89.21 $\pm$ 0.7	81.63 $\pm$ 0.6	96.19 $\pm$ 0.4	96.68 $\pm$ 0.2	83.35 $\pm$ 0.9	84.82 $\pm$ 1.2	86.39 $\pm$ 1.8	64.89 $\pm$ 1.1	71.13 $\pm$ 1.4	71.13 $\pm$ 1.4	68.39 $\pm$ 1.0	64.89 $\pm$ 1.1	71.13 $\pm$ 1.4	66.07 $\pm$ 1.5	73.44 $\pm$ 1.4			
			Projection	97.83 $\pm$ 0.1	99.29 $\pm$ 0.0	89.28 $\pm$ 0.8	91.85 $\pm$ 0.3	96.79 $\pm$ 0.2	98.14 $\pm$ 0.1	84.49 $\pm$ 1.0	93.17 $\pm$ 0.7	87.09 $\pm$ 0.4	66.07 $\pm$ 1.5	73.44 $\pm$ 1.4	73.44 $\pm$ 1.4	66.07 $\pm$ 1.5	73.44 $\pm$ 1.4	73.44 $\pm$ 1.4	66.07 $\pm$ 1.5	73.44 $\pm$ 1.4			
331 332 333 334 335 336 337 338 339 340 341 342 343 344 345 346 347 348 349	331 332 333 334 335 336 337 338 339 340 341 342 343 344 345 346 347 348 349	331 332 333 334 335 336 337 338 339 340 341 342 343 344 345 346 347 348 349	Baseline	98.83 $\pm$ 0.1	99.04 $\pm$ 0.0	89.64 $\pm$ 0.9	87.85 $\pm$ 0.9	98.45 $\pm$ 0.1	98.39 $\pm$ 0.1	89.51 $\pm$ 0.7	90.14 $\pm$ 1.0	83.98 $\pm$ 3.4	65.36 $\pm$ 2.9	69.61 $\pm$ 2.5	68.18 $\pm$ 0.5	62.13 $\pm$ 2.0	70.57 $\pm$ 1.1	70.57 $\pm$ 1.1	68.18 $\pm$ 0.5	62.13 $\pm$ 2.0	70.57 $\pm$ 1.1	68.18 $\pm$ 0.5	70.57 $\pm$ 1.1
			Vanilla	98.75 $\pm$ 0.0	98.88 $\pm$ 0.0	88.91 $\pm$ 0.4	89.54 $\pm$ 0.3	98.22 $\pm$ 0.0	97.73 $\pm$ 0.0	88.22 $\pm$ 0.3	90.78 $\pm$ 0.0	86.18 $\pm$ 0.5	62.13 $\pm$ 2.0	70.57 $\pm$ 1.1	70.57 $\pm$ 1.1	68.18 $\pm$ 0.5	62.13 $\pm$ 2.0	70.57 $\pm$ 1.1	68.18 $\pm$ 0.5	70.57 $\pm$ 1.1			
			Transformer	98.95 $\pm$ 0.0	99.25 $\pm$ 0.0	91.10 $\pm$ 0.4	90.63 $\pm$ 0.3	98.52 $\pm$ 0.1	98.68 $\pm$ 0.0	88.82 $\pm$ 0.9	91.71 $\pm$ 0.2	82.02 $\pm$ 7.0	61.41 $\pm$ 2.6	71.44 $\pm$ 0.6	71.44 $\pm$ 0.6	68.82 $\pm$ 0.9	61.41 $\pm$ 2.6	71.44 $\pm$ 0.6	68.82 $\pm$ 0.9	71.44 $\pm$ 0.6			
			Projection	99.10 $\pm$ 0.1	99.47 $\pm$ 0.0	90.94 $\pm$ 0.2	95.21 $\pm$ 0.2	97.85 $\pm$ 0.1	99.07 $\pm$ 0.0	89.61 $\pm$ 0.4	95.81 $\pm$ 0.1	86.65 $\pm$ 0.9	60.75 $\pm$ 1.3	75.18 $\pm$ 2.1	75.18 $\pm$ 2.1	60.75 $\pm$ 1.3	75.18 $\pm$ 2.1	75.18 $\pm$ 2.1	60.75 $\pm$ 1.3	75.18 $\pm$ 2.1			
331 332 333 334 335 336 337 338 339 340 341 342 343 344 345 346 347 348 349	331 332 333 334 335 336 337 338 339 340 341 342 343 344 345 346 347 348 349	331 332 333 334 335 336 337 338 339 340 341 342 343 344 345 346 347 348 349	Baseline	98.90 $\pm$ 0.0	99.02 $\pm$ 0.0	86.99 $\pm$ 1.6	82.78 $\pm$ 0.2	98.58 $\pm$ 0.0	98.59 $\pm$ 0.0	86.42 $\pm$ 1.7	89.11 $\pm$ 0.3	80.84 $\pm$ 4.6	62.58 $\pm$ 1.3	64.91 $\pm$ 5.2	68.68 $\pm$ 1.9	63.16 $\pm$ 1.4	70.16 $\pm$ 1.1	70.16 $\pm$ 1.1	68.68 $\pm$ 1.9	63.16 $\pm$ 1.4	70.16 $\pm$ 1.1	68.68 $\pm$ 1.9	
			Vanilla	98.89 $\pm$ 0.0	98.90 $\pm$ 0.0	87.43 $\pm$ 0.4	86.13 $\pm$ 0.4	98.50 $\pm$ 0.0	98.33 $\pm$ 0.0	87.28 $\pm$ 1.5	88.18 $\pm$ 0.5	85.12 $\pm$ 0.3	63.16 $\pm$ 1.4	70.16 $\pm$ 1.1	70.16 $\pm$ 1.1	68.68 $\pm$ 1.9	63.16 $\pm$ 1.4	70.16 $\pm$ 1.1	68.68 $\pm$ 1.9	70.16 $\pm$ 1.1			
			Transformer	98.98 $\pm$ 0.0	99.22 $\pm$ 0.0	90.31 $\pm$ 0.4	88.22 $\pm$ 0.4	98.59 $\pm$ 0.0	98.88 $\pm$ 0.0	89.05 $\pm$ 1.0	90.69 $\pm$ 0.4	77.15 $\pm$ 8.9	61.94 $\pm$ 2.1	71.26 $\pm$ 1.2	71.26 $\pm$ 1.2	68.68 $\pm$ 1.9	61.94 $\pm$ 2.1	71.26 $\pm$ 1.2	68.68 $\pm$ 1.9	71.26 $\pm$ 1.2			
			Projection	99.16 $\pm$ 0.0	99.49 $\pm$ 0.0	89.74 $\pm$ 0.5	93.73 $\pm$ 0.2	98.89 $\pm$ 0.0	99.26 $\pm$ 0.0	89.42 $\pm$ 1.5	95.07 $\pm$ 0.3	86.30 $\pm$ 0.8	62.75 $\pm$ 1.5	74.07 $\pm$ 0.5	74.07 $\pm$ 0.5	62.75 $\pm$ 1.5	74.07 $\pm$ 0.5	74.07 $\pm$ 0.5	62.75 $\pm$ 1.5	74.07 $\pm$ 0.5			
331 332 333 334 335 336 337 338 339 340 341 342 343 344 345 346 347 348 349	331 332 333 334 335 336 337 338 339 340 341 342 343 344 345 346 347 348 349	331 332 333 334 335 336 337 338 339 340 341 342 343 344 345 346 347 348 349	Baseline	97.25 $\pm$ 0.0	97.31 $\pm$ 0.0	82.78 $\pm$ 0.2	75.61 $\pm$ 0.2	96.65 $\pm$ 0.0	95.26 $\pm$ 0.0	81.41 $\pm$ 0.2	82.11 $\pm$ 0.4	86.80 $\pm$ 0.8	64.22 $\pm$ 3.3	69.42 $\pm$ 0.8	68.68 $\pm$ 1.9	68.92 $\pm$ 1.5	69.77 $\pm$ 0.8	70.91 $\pm$ 0.5	70.91 $\pm$ 0.5	68.68 $\pm$ 1.9	70.91 $\pm$ 0.5	70.91 $\pm$ 0.5	
			Vanilla	96.12 $\pm$ 0.0	92.95 $\pm$ 0.3	80.86 $\pm$ 0.6	76.57 $\pm$ 1.5	95.56 $\pm$ 0.0	94.33 $\pm$ 0.2	78.28 $\pm$ 1.1	75.73 $\pm$ 2.5	89.00 $\pm$ 0.0	69.77 $\pm$ 0.8	70.91 $\pm$ 0.5	70.91 $\pm$ 0.5	68.68 $\pm$ 1.9	69.77 $\pm$ 0.8	70.91 $\pm$ 0.5	68.68 $\pm$ 1.9	70.91 $\pm$ 0.5	70.91 $\pm$ 0.5		
			Transformer	97.39 $\pm$ 0.0	98.28 $\pm$ 0.0	84.44 $\pm$ 0.4	79.28 $\pm$ 0.1	96.98 $\pm$ 0.1	96.67 $\pm$ 0.0	82.14 $\pm$ 0.8	84.39 $\pm$ 0.2	88.24<math											

378  
 379 Table 2: The results for the link prediction task under the “pre-train, prompt” paradigm, note that  
 380 **only 20% of data is used** in total (10% for pre-train, 10% for fine-tune). Results colored in **blue**  
 381 indicate that they **even surpass** the baseline achieved with **70% of the data used** for training.

		Only 20% of data used				Transductive Link Prediction				Inductive Link Prediction					
		TProG	Wikipedia	Reddit	MOOC	LastFM	Wikipedia	Reddit	MOOC	LastFM	Wikipedia	Reddit	MOOC		
382 383 384 385 386 387 388 389 390 391 392 393 394 395 396 397 398 399 400 401 402 403 404 405 406 407 408 409 410 411 412 413 414 415 416 417 418 419 420 421 422 423 424 425 426 427 428 429 430 431	382 383 384 385 386 387 388 389 390 391 392 393 394 395 396 397 398 399 400 401 402 403 404 405 406 407 408 409 410 411 412 413 414 415 416 417 418 419 420 421 422 423 424 425 426 427 428 429 430 431	Baseline	79.28 $\pm$ 4.2	92.39 $\pm$ 1.4	55.73 $\pm$ 2.2	68.00 $\pm$ 0.7	79.30 $\pm$ 4.8	80.58 $\pm$ 2.8	58.51 $\pm$ 2.6	80.96 $\pm$ 1.3	Baseline	79.20 $\pm$ 0.7	80.58 $\pm$ 0.7	58.51 $\pm$ 2.6	
		Vanilla	89.17 $\pm$ 0.4	96.39 $\pm$ 0.1	63.10 $\pm$ 0.2	72.57 $\pm$ 1.0	88.00 $\pm$ 0.6	94.33 $\pm$ 0.1	63.52 $\pm$ 0.3	Vanilla	89.17 $\pm$ 0.7	94.33 $\pm$ 0.1	63.52 $\pm$ 0.3		
		Transformer	92.11 $\pm$ 0.9	97.54 $\pm$ 0.0	72.98 $\pm$ 0.3	77.99 $\pm$ 0.6	92.34 $\pm$ 0.7	96.43 $\pm$ 0.0	73.25 $\pm$ 0.3	Transformer	92.11 $\pm$ 0.9	96.43 $\pm$ 0.0	73.25 $\pm$ 0.3		
		Projection	95.64 $\pm$ 0.3	98.54 $\pm$ 0.1	76.23 $\pm$ 0.3	89.21 $\pm$ 0.1	95.04 $\pm$ 0.2	97.71 $\pm$ 0.1	76.31 $\pm$ 0.3	Projection	95.64 $\pm$ 0.3	97.71 $\pm$ 0.1	76.31 $\pm$ 0.3		
382 383 384 385 386 387 388 389 390 391 392 393 394 395 396 397 398 399 400 401 402 403 404 405 406 407 408 409 410 411 412 413 414 415 416 417 418 419 420 421 422 423 424 425 426 427 428 429 430 431	382 383 384 385 386 387 388 389 390 391 392 393 394 395 396 397 398 399 400 401 402 403 404 405 406 407 408 409 410 411 412 413 414 415 416 417 418 419 420 421 422 423 424 425 426 427 428 429 430 431	DyRep	Baseline	88.19 $\pm$ 1.0	96.82 $\pm$ 0.3	73.13 $\pm$ 1.7	67.38 $\pm$ 1.1	85.99 $\pm$ 0.9	92.01 $\pm$ 0.8	71.91 $\pm$ 1.1	79.67 $\pm$ 1.8	Baseline	88.19 $\pm$ 1.0	92.01 $\pm$ 0.8	71.91 $\pm$ 1.1
		Vanilla	84.27 $\pm$ 1.2	96.35 $\pm$ 0.1	61.19 $\pm$ 1.3	69.85 $\pm$ 0.5	83.93 $\pm$ 0.9	93.82 $\pm$ 0.3	61.42 $\pm$ 1.5	Vanilla	84.27 $\pm$ 1.2	93.82 $\pm$ 0.3	61.42 $\pm$ 1.5		
		Transformer	91.68 $\pm$ 0.4	97.40 $\pm$ 0.1	72.44 $\pm$ 1.0	74.78 $\pm$ 0.4	91.23 $\pm$ 0.5	96.28 $\pm$ 0.2	72.75 $\pm$ 1.0	Transformer	91.68 $\pm$ 0.4	96.28 $\pm$ 0.2	72.75 $\pm$ 1.0		
		Projection	95.74 $\pm$ 0.2	98.63 $\pm$ 0.0	76.40 $\pm$ 0.2	88.26 $\pm$ 0.2	95.40 $\pm$ 0.2	97.74 $\pm$ 0.1	76.40 $\pm$ 0.3	Projection	95.74 $\pm$ 0.2	97.74 $\pm$ 0.1	76.40 $\pm$ 0.3		
382 383 384 385 386 387 388 389 390 391 392 393 394 395 396 397 398 399 400 401 402 403 404 405 406 407 408 409 410 411 412 413 414 415 416 417 418 419 420 421 422 423 424 425 426 427 428 429 430 431	382 383 384 385 386 387 388 389 390 391 392 393 394 395 396 397 398 399 400 401 402 403 404 405 406 407 408 409 410 411 412 413 414 415 416 417 418 419 420 421 422 423 424 425 426 427 428 429 430 431	TGN	Baseline	96.34 $\pm$ 0.2	97.63 $\pm$ 0.1	56.54 $\pm$ 0.5	66.54 $\pm$ 2.0	95.86 $\pm$ 0.3	95.98 $\pm$ 0.4	61.11 $\pm$ 0.9	75.09 $\pm$ 2.8	Baseline	96.34 $\pm$ 0.2	95.98 $\pm$ 0.4	61.11 $\pm$ 0.9
		Vanilla	95.59 $\pm$ 0.1	97.63 $\pm$ 0.1	74.30 $\pm$ 1.2	64.36 $\pm$ 2.0	95.27 $\pm$ 0.2	96.32 $\pm$ 0.2	74.58 $\pm$ 1.1	Vanilla	95.59 $\pm$ 0.1	96.32 $\pm$ 0.2	74.58 $\pm$ 1.1		
		Transformer	96.23 $\pm$ 0.1	98.09 $\pm$ 0.0	75.15 $\pm$ 0.8	67.65 $\pm$ 3.0	95.79 $\pm$ 0.1	97.35 $\pm$ 0.1	75.25 $\pm$ 0.7	Transformer	96.23 $\pm$ 0.1	97.35 $\pm$ 0.1	75.25 $\pm$ 0.7		
		Projection	96.93 $\pm$ 0.2	98.95 $\pm$ 0.0	79.10 $\pm$ 0.6	87.42 $\pm$ 0.4	96.58 $\pm$ 0.3	98.38 $\pm$ 0.1	79.17 $\pm$ 0.5	Projection	96.93 $\pm$ 0.2	98.38 $\pm$ 0.1	79.17 $\pm$ 0.5		
382 383 384 385 386 387 388 389 390 391 392 393 394 395 396 397 398 399 400 401 402 403 404 405 406 407 408 409 410 411 412 413 414 415 416 417 418 419 420 421 422 423 424 425 426 427 428 429 430 431	382 383 384 385 386 387 388 389 390 391 392 393 394 395 396 397 398 399 400 401 402 403 404 405 406 407 408 409 410 411 412 413 414 415 416 417 418 419 420 421 422 423 424 425 426 427 428 429 430 431	TIGE	Baseline	98.36 $\pm$ 0.1	98.71 $\pm$ 0.1	80.60 $\pm$ 1.5	84.73 $\pm$ 0.7	98.11 $\pm$ 0.1	98.46 $\pm$ 0.1	80.71 $\pm$ 1.4	85.73 $\pm$ 0.8	Baseline	98.36 $\pm$ 0.1	98.46 $\pm$ 0.1	80.71 $\pm$ 1.4
		Vanilla	98.50 $\pm$ 0.0	98.58 $\pm$ 0.0	80.58 $\pm$ 0.4	85.24 $\pm$ 0.3	98.20 $\pm$ 0.0	98.16 $\pm$ 0.0	80.88 $\pm$ 0.3	Vanilla	98.50 $\pm$ 0.0	98.16 $\pm$ 0.0	80.88 $\pm$ 0.3		
		Transformer	98.92 $\pm$ 0.0	99.08 $\pm$ 0.0	80.32 $\pm$ 1.2	87.77 $\pm$ 0.4	98.69 $\pm$ 0.0	98.90 $\pm$ 0.0	80.56 $\pm$ 1.1	Transformer	98.92 $\pm$ 0.0	98.90 $\pm$ 0.0	80.56 $\pm$ 1.1		
		Projection	98.82 $\pm$ 0.0	99.32 $\pm$ 0.0	83.11 $\pm$ 0.1	93.40 $\pm$ 0.2	98.63 $\pm$ 0.0	99.16 $\pm$ 0.0	83.30 $\pm$ 0.1	Projection	98.82 $\pm$ 0.0	99.16 $\pm$ 0.0	83.30 $\pm$ 0.1		
382 383 384 385 386 387 388 389 390 391 392 393 394 395 396 397 398 399 400 401 402 403 404 405 406 407 408 409 410 411 412 413 414 415 416 417 418 419 420 421 422 423 424 425 426 427 428 429 430 431	382 383 384 385 386 387 388 389 390 391 392 393 394 395 396 397 398 399 400 401 402 403 404 405 406 407 408 409 410 411 412 413 414 415 416 417 418 419 420 421 422 423 424 425 426 427 428 429 430 431	TIGER	Baseline	98.32 $\pm$ 0.1	98.67 $\pm$ 0.1	80.31 $\pm$ 0.6	84.53 $\pm$ 0.4	98.10 $\pm$ 0.1	98.12 $\pm$ 0.2	78.07 $\pm$ 0.5	88.54 $\pm$ 0.5	Baseline	98.32 $\pm$ 0.1	98.12 $\pm$ 0.2	78.07 $\pm$ 0.5
		Vanilla	98.50 $\pm$ 0.0	98.62 $\pm$ 0.0	80.47 $\pm$ 0.3	84.66 $\pm$ 0.1	98.22 $\pm$ 0.0	98.31 $\pm$ 0.0	80.88 $\pm$ 0.3	Vanilla	98.50 $\pm$ 0.0	98.31 $\pm$ 0.0	80.88 $\pm$ 0.3		
		Transformer	95.55 $\pm$ 0.2	97.48 $\pm$ 0.1	82.71 $\pm$ 0.8	78.39 $\pm$ 0.1	95.30 $\pm$ 0.1	96.71 $\pm$ 0.1	82.67 $\pm$ 0.8	Transformer	95.55 $\pm$ 0.2	96.71 $\pm$ 0.1	82.67 $\pm$ 0.8		
		Projection	98.80 $\pm$ 0.2	98.91 $\pm$ 0.1	87.05 $\pm$ 2.0	83.67 $\pm$ 3.5	97.44 $\pm$ 0.5	96.13 $\pm$ 0.3	86.68 $\pm$ 1.9	Projection	98.80 $\pm$ 0.2	96.13 $\pm$ 0.3	86.68 $\pm$ 1.9		
382 383 384 385 386 387 388 389 390 391 392 393 394 395 396 397 398 399 400 401 402 403 404 405 406 407 408 409 410 411 412 413 414 415 416 417 418 419 420 421 422 423 424 425 426 427 428 429 430 431	382 383 384 385 386 387 388 389 390 391 392 393 394 395 396 397 398 399 400 401 402 403 404 405 406 407 408 409 410 411 412 413 414 415 416 417 418 419 420 421 422 423 424 425 426 427 428 429 430 431	GraphMixer	Baseline	95.88 $\pm$ 0.1	96.51 $\pm$ 0.0	75.65 $\pm$ 1.5	74.14 $\pm$ 0.4	95.61 $\pm$ 0.0	94.43 $\pm$ 0.0	74.10 $\pm$ 1.6	80.84 $\pm$ 0.6	Baseline	95.88 $\pm$ 0.1	94.43 $\pm$ 0.0	74.10 $\pm$ 1.6
		Vanilla	94.41 $\pm$ 0.1	96.32 $\pm$ 0.1	73.34 $\pm$ 2.2	77.30 $\pm$ 0.2	93.80 $\pm$ 0.1	94.77 $\pm$ 0.1	73.28 $\pm$ 2.2	Vanilla	94.41 $\pm$ 0.1	94.77 $\pm$ 0.1	73.28 $\pm$ 2.2		
		Transformer	95.55 $\pm$ 0.2	97.48 $\pm$ 0.1	82.71 $\pm$ 0.8	78.39 $\pm$ 0.1	95.30 $\pm$ 0.1	96.71 $\pm$ 0.1	82.67 $\pm$ 0.8	Transformer	95.55 $\pm$ 0.2	96.71 $\pm$ 0.1	82.67 $\pm$ 0.8		
		Projection	98.80 $\pm$ 0.2	98.91 $\pm$ 0.1	87.05 $\pm$ 2.0	83.67 $\pm$ 3.5	97.44 $\pm$ 0.5	96.13 $\pm$ 0.3	86.68 $\pm$ 1.9	Projection	98.80 $\pm$ 0.2	96.13 $\pm$ 0.3	86.68 $\pm$ 1.9		
382 383 384 385 386 387 388 389 390 391 392 393 394 395 396 397 398 399 400 401 402 403 404 405 406 407 408 409 410 411 412 413 414 415 416 417 418 419 420 421 422 423 424 425 426 427 428 429 430 431	382 383 384 385 386 387 388 389 390 391 392 393 394 395 396 397 398 399 400 401 402 403 404 405 406 407 408 409 410 411 412 413 414 415<br														

432 4.4 “PRE-TRAIN, PROMPT-BASED FINE-TUNE”  
433434 In the “pre-train, prompt-based fine-tune” paradigm, we follow a similar experimental setting as with  
435 “pre-train, prompt”, with a key difference: instead of freezing the pre-trained model’s parameters,  
436 we allow for their simultaneous optimization while using 20% of the data to train the TProG. This  
437 adjustment aims to enhance the model’s adaptability to new data and downstream tasks. The full  
438 experimental results are shown in Appendix D. As shown in Tab. 6, this paradigm yields improved  
439 results compared to “pre-train, prompt” on link prediction task, attributable to the fine-tuning of the  
440 pre-trained model. However, this approach requires more training resources due to the optimization  
441 of the pre-trained model’s parameters. Thus, this training paradigm is recommended when sufficient  
442 resources are available to achieve optimal results. More details of node classification task are  
443 discussed in Appendix D.2.  
444445 4.5 COMPARISON WITH EXISTING GRAPH PROMPTS  
446447 As discussed in Sec. 3.4, we conduct experiments using prompts from static graphs, i.e., GraphPrompt  
448 (Liu et al., 2023b) and GPF (Fang et al., 2023), where a single, learnable prompt vector is applied  
449 uniformly across all nodes, either on the input (Fang et al., 2023) or on the output (Liu et al., 2023b)  
450 embeddings. The comparative results of these experiments are depicted in Fig. 4. The results  
451 demonstrate that our method significantly outperforms the traditional prompt method used in static  
452 graphs, demonstrating our effectiveness once again.  
453454 4.6 EFFECTIVENESS OF VARIOUS TPROGS  
455456 As indicated in Tab. 1 and 6, the Projection TProG generally outperforms other types of TProG in  
457 link prediction tasks, with the Transformer TProG also excelling in certain scenarios. In contrast, the  
458 Vanilla TProG often shows weaker performance, likely due to its limited capacity to express temporal  
459 information. However, in node classification tasks, the Vanilla TProG demonstrates improved results  
460 on specific datasets. Meanwhile, the Projection TProG consistently surpasses the baseline, though  
461 the Transformer TProG shows slightly lower effectiveness.  
462463 The Transformer TProG captures recent behavior patterns, whereas the Projection TProG emphasizes  
464 the global historical state. The scenarios where the Transformer TProG demonstrates superior  
465 performance are predominantly observed on the MOOC dataset. This suggests that the recent  
466 behavioral characteristics inherent to this dataset are particularly effective in bridging the existing  
467 gaps. The robust performance of the Projection TProG across various tasks can be ascribed to its  
468 ability to model global historical information, which possesses significant expressive power for  
469 capturing temporal dynamics in TIGs. Additionally, its node-specific learnable embeddings play a  
470 pivotal role in effectively bridging the semantic gap between pretext and downstream tasks.  
471472 Although the Transformer and Projection TProG generally exhibit stronger temporal expressiveness,  
473 there remain cases, particularly in node classification task, where the simpler Vanilla TProG performs  
474 competitively or even slightly better. This phenomenon is consistent with the distinct nature of  
475 node classification, which typically depends more on semantic alignment than on detailed temporal  
476 dynamics. As analyzed earlier, the semantic gap arising from the mismatch between link-level  
477 pretext training and node-level downstream objectives often becomes the primary bottleneck for  
478 node classification. The Vanilla TProG introduces node-specific learnable embeddings that directly  
479 encode task-relevant semantic information without additional temporal modeling. In datasets such as  
480 Reddit, where interactions are dense and long-term temporal dependencies are relatively weak, this  
481 lightweight semantic adaptation proves particularly effective, leading to performance that rivals or  
482 occasionally surpasses more expressive variants.  
483484 **Source of the Performance Improving.** As shown in Tab. 1, the Vanilla TProG, without using  
485 the temporal information, generally exhibits inferior performance in link prediction tasks compared  
486 to the Transformer and Projection TProG, both of which incorporate time-related prompts. This  
487 demonstrates that adding time-related information contributes to performance enhancement. Furthermore,  
488 our comparison with static graph methods in Sec. 4.5, indirectly corroborates that the observed  
489 improvements are attributable to the proposed TProG.  
490

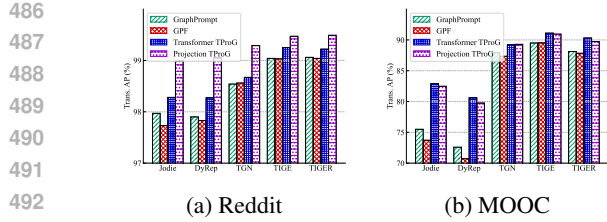


Figure 4: Comparison between traditional prompt on static graphs (Liu et al., 2023b; Fang et al., 2023) and our methods (“pre-train, prompt” paradigm, transductive link prediction on Reddit and MOOC).

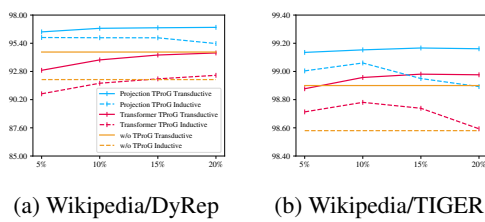


Figure 5: Performance w.r.t the Proportion of Prompting Data. This figure is continued in Appendix E.1, Fig. 7.

## 4.7 PERFORMANCE WITH LIMITED DATA

### 4.7.1 PERFORMANCE WITH LIMITED TRAINING DATA

To validate the effectiveness of the proposed prompt method and demonstrate that it requires only a small dataset to achieve superior results, we strategically design an experiment using merely 10% of the data for pre-training, followed by another 10% for prompt tuning (“pre-train, prompt”). As a baseline for comparison, we utilized the results reported in TIGE (Zhang et al., 2023c), which is trained on only 20% of the data. The experimental outcomes, detailed in Tab. 2, clearly illustrate that our method, even with limited data for training and prompt tuning, can attain the best results among all the baselines. Remarkably, on certain dataset/model combinations, our results even surpass the baseline achieved with 70% of the data used for training.

### 4.7.2 PERFORMANCE WITH LIMITED PROMPT DATA

To further explore the efficiency of our method, we investigate the minimum amount of data required for prompt tuning to surpass baseline performances. We utilize 50% of the data for pre-training, and 5% to 20% data for prompt tuning. We select DyRep (Trivedi et al., 2019) and TIGER (Zhang et al., 2023c) to conduct experiments under the “pre-train, prompt” paradigm for this analysis. The results, as depicted in Fig. 5 and Fig. 7, reveal that as little as 10%, and in some cases only 5%, of the data is needed for our approach to prompt tuning to achieve improved results. Furthermore, we observe that increasing the amount of data used for prompt tuning correspondingly enhances the performances in the transductive setting. This finding reaffirms the efficacy of our approach.

## 5 CONCLUSION

In this paper, we introduce two novel training paradigms for TIGs, which are grounded in pre-training, prompting, and fine-tuning techniques. Additionally, we present and compare three distinct temporal prompt generators, designed to ensure the resulting prompt vectors encapsulate a significant amount of temporal information. Employing the proposed paradigms can bridge both temporal and semantic gaps in the traditional training paradigm. Moreover, through extensive experimentation, we demonstrate that our methods significantly improve the performance of TIG models over baselines across various downstream tasks, thus achieving SOTA performance.

## REFERENCES

Christopher M Bishop and Nasser M Nasrabadi. *Pattern recognition and machine learning*, volume 4. Springer, 2006.

Mouxiang Chen, Zemin Liu, Chenghao Liu, Jundong Li, Qiheng Mao, and Jianling Sun. Ultra-dp: Unifying graph pre-training with multi-task graph dual prompt. *arXiv preprint arXiv:2310.14845*, 2023a.

540    Xi Chen, Yongxiang Liao, Yun Xiong, Yao Zhang, Siwei Zhang, Jiawei Zhang, and Yiheng Sun.  
 541    Speed: Streaming partition and parallel acceleration for temporal interaction graph embedding.  
 542    *arXiv preprint arXiv:2308.14129*, 2023b.  
 543

544    Weilin Cong, Si Zhang, Jian Kang, Baichuan Yuan, Hao Wu, Xin Zhou, Hanghang Tong, and  
 545    Mehrdad Mahdavi. Do we really need complicated model architectures for temporal networks? In  
 546    *The Eleventh International Conference on Learning Representations*, 2023.

547    Hanjun Dai, Yichen Wang, Rakshit Trivedi, and Le Song. Deep coevolutionary network: Embedding  
 548    user and item features for recommendation. *arXiv preprint arXiv:1609.03675*, 2016.

549

550    Jacob Devlin, Ming-Wei Chang, Kenton Lee, and Kristina Toutanova. Bert: Pre-training of deep  
 551    bidirectional transformers for language understanding. *arXiv preprint arXiv:1810.04805*, 2018.

552

553    Zifeng Ding, Yifeng Li, Yuan He, Antonio Norelli, Jingcheng Wu, Volker Tresp, Michael Bronstein,  
 554    and Yunpu Ma. Dygmamba: Efficiently modeling long-term temporal dependency on continuous-  
 555    time dynamic graphs with state space models. *arXiv preprint arXiv:2408.04713*, 2024.

556    Taoran Fang, Yunchao Zhang, Yang Yang, Chunping Wang, and Lei Chen. Universal prompt tuning  
 557    for graph neural networks. In *Thirty-seventh Conference on Neural Information Processing  
 558    Systems*, 2023.

559

560    Qingqing Ge, Zeyuan Zhao, Yiding Liu, Anfeng Cheng, Xiang Li, Shuaiqiang Wang, and Dawei Yin.  
 561    Enhancing graph neural networks with structure-based prompt. *arXiv preprint arXiv:2310.17394*,  
 562    2023.

563

564    Chenghua Gong, Xiang Li, Jianxiang Yu, Cheng Yao, Jiaqi Tan, Chengcheng Yu, and Dawei Yin.  
 565    Prompt tuning for multi-view graph contrastive learning. *arXiv preprint arXiv:2310.10362*, 2023.

566    Junfeng Hu, Xu Liu, Zhencheng Fan, Yifang Yin, Shili Xiang, Savitha Ramasamy, and Roger  
 567    Zimmermann. Prompt-based spatio-temporal graph transfer learning. In *Proceedings of the 33rd  
 568    ACM International Conference on Information and Knowledge Management*, pp. 890–899, 2024.

569

570    Qian Huang, Hongyu Ren, Peng Chen, Gregor Kržmanc, Daniel Zeng, Percy Liang, and Jure  
 571    Leskovec. Prodigy: Enabling in-context learning over graphs. In *Thirty-seventh Conference on  
 572    Neural Information Processing Systems*, 2023a.

573

574    Shenyang Huang, Farimah Poursafaei, Jacob Danovitch, Matthias Fey, Weihua Hu, Emanuele Rossi,  
 575    Jure Leskovec, Michael Bronstein, Guillaume Rabusseau, and Reihaneh Rabbany. Temporal graph  
 576    benchmark for machine learning on temporal graphs. *Advances in Neural Information Processing  
 577    Systems*, 36:2056–2073, 2023b.

578    Srijan Kumar, Xikun Zhang, and Jure Leskovec. Predicting dynamic embedding trajectory in  
 579    temporal interaction networks. In *Proceedings of the 25th ACM SIGKDD international conference  
 580    on knowledge discovery & data mining*, pp. 1269–1278, 2019.

581    Pengfei Liu, Weizhe Yuan, Jinlan Fu, Zhengbao Jiang, Hiroaki Hayashi, and Graham Neubig.  
 582    Pre-train, prompt, and predict: A systematic survey of prompting methods in natural language  
 583    processing. *ACM Computing Surveys*, 55(9):1–35, 2023a.

584

585    Zemin Liu, Xingtong Yu, Yuan Fang, and Xinming Zhang. Graphprompt: Unifying pre-training and  
 586    downstream tasks for graph neural networks. In *Proceedings of the ACM Web Conference 2023*,  
 587    pp. 417–428, 2023b.

588    Yihong Ma, Ning Yan, Jiayu Li, Masood Mortazavi, and Nitesh V Chawla. Hetgpt: Harnessing the  
 589    power of prompt tuning in pre-trained heterogeneous graph neural networks. In *Proceedings of the  
 590    ACM on Web Conference 2024*, pp. 1015–1023, 2024.

591

592    Guanghui Qin and Jason Eisner. Learning how to ask: Querying lms with mixtures of soft prompts.  
 593    In *Proceedings of the 2021 Conference of the North American Chapter of the Association for  
 Computational Linguistics: Human Language Technologies (NAACL-HLT)*, 2021.

594 Emanuele Rossi, Ben Chamberlain, Fabrizio Frasca, Davide Eynard, Federico Monti, and Michael  
 595 Bronstein. Temporal graph networks for deep learning on dynamic graphs. *arXiv preprint*  
 596 *arXiv:2006.10637*, 2020.

597

598 Reza Shirkavand and Heng Huang. Deep prompt tuning for graph transformers. *arXiv preprint*  
 599 *arXiv:2309.10131*, 2023.

600

601 Mingchen Sun, Kaixiong Zhou, Xin He, Ying Wang, and Xin Wang. Gppt: Graph pre-training and  
 602 prompt tuning to generalize graph neural networks. In *Proceedings of the 28th ACM SIGKDD*  
 603 *Conference on Knowledge Discovery and Data Mining*, pp. 1717–1727, 2022.

604

605 Xiangguo Sun, Hong Cheng, Jia Li, Bo Liu, and Jihong Guan. All in one: Multi-task prompting  
 606 for graph neural networks. In *Proceedings of the 29th ACM SIGKDD Conference on Knowledge*  
 607 *Discovery and Data Mining*, pp. 2120–2131, 2023.

608

609 Zhen Tan, Ruocheng Guo, Kaize Ding, and Huan Liu. Virtual node tuning for few-shot node  
 610 classification. In *Proceedings of the 29th ACM SIGKDD Conference on Knowledge Discovery and*  
 611 *Data Mining*, pp. 2177–2188, 2023.

612

613 Yuxing Tian, Yiyan Qi, and Fan Guo. Freedyg: Frequency enhanced continuous-time dynamic graph  
 614 model for link prediction. In *The twelfth international conference on learning representations*,  
 615 2024.

616

617 Rakshit Trivedi, Mehrdad Farajtabar, Prasenjeet Biswal, and Hongyuan Zha. Dyrep: Learning  
 618 representations over dynamic graphs. In *The Seventh International Conference on Learning*  
 619 *Representations*, 2019.

620

621 Maria Tsimpoukelli, Jacob L Menick, Serkan Cabi, SM Eslami, Oriol Vinyals, and Felix Hill.  
 622 Multimodal few-shot learning with frozen language models. *Advances in Neural Information*  
 623 *Processing Systems*, 34:200–212, 2021.

624

625 Ashish Vaswani, Noam Shazeer, Niki Parmar, Jakob Uszkoreit, Llion Jones, Aidan N Gomez, Łukasz  
 626 Kaiser, and Illia Polosukhin. Attention is all you need. *Advances in neural information processing*  
 627 *systems*, 30, 2017.

628

629 Da Xu, Chuanwei Ruan, Evren Korpeoglu, Sushant Kumar, and Kannan Achan. Inductive rep-  
 630 resentation learning on temporal graphs. In *The Eighth International Conference on Learning*  
 631 *Representations*, 2020.

632

633 Le Yu, Leilei Sun, Bowen Du, and Weifeng Lv. Towards better dynamic graph learning: New  
 634 architecture and unified library. *Advances in Neural Information Processing Systems*, 36:67686–  
 635 67700, 2023.

636

637 Xingtong Yu, Yuan Fang, Zemin Liu, and Xinming Zhang. Hgprompt: Bridging homogeneous and  
 638 heterogeneous graphs for few-shot prompt learning. In *Proceedings of the AAAI Conference on*  
 639 *Artificial Intelligence*, volume 38, pp. 16578–16586, 2024a.

640

641 Xingtong Yu, Zhenghao Liu, Yuan Fang, Zemin Liu, Sihong Chen, and Xinming Zhang. Generalized  
 642 graph prompt: Toward a unification of pre-training and downstream tasks on graphs. *IEEE*  
 643 *Transactions on Knowledge and Data Engineering*, 2024b.

644

645 Xingtong Yu, Jie Zhang, Yuan Fang, and Renhe Jiang. Non-homophilic graph pre-training and  
 646 prompt learning. *arXiv preprint arXiv:2408.12594*, 2024c.

647

648 Xingtong Yu, Zhenghao Liu, Xinming Zhang, and Yuan Fang. Node-time conditional prompt learning  
 649 in dynamic graphs. In *The Thirteenth International Conference on Learning Representations*, 2025.  
 650 URL <https://openreview.net/forum?id=kV1fYvIqaK>.

651

652 Siwei Zhang, Yun Xiong, Yao Zhang, Yiheng Sun, Xi Chen, Yizhu Jiao, and Yangyong Zhu. Rdgsl:  
 653 Dynamic graph representation learning with structure learning. In *Proceedings of the 32nd ACM*  
 654 *International Conference on Information and Knowledge Management*, pp. 3174–3183, 2023a.

648 Siwei Zhang, Yun Xiong, Yao Zhang, Xixi Wu, Yiheng Sun, and Jiawei Zhang. ilore: Dynamic graph  
649 representation with instant long-term modeling and re-occurrence preservation. In *Proceedings*  
650 of the 32nd ACM International Conference on Information and Knowledge Management, pp.  
651 3216–3225, 2023b.

652 Yao Zhang, Yun Xiong, Xiangnan Kong, and Yangyong Zhu. Learning node embeddings in inter-  
653 action graphs. In *Proceedings of the 2017 ACM on Conference on Information and Knowledge*  
654 *Management*, pp. 397–406, 2017.

655 Yao Zhang, Yun Xiong, Yongxiang Liao, Yiheng Sun, Yucheng Jin, Xuehao Zheng, and Yangyong  
656 Zhu. Tiger: Temporal interaction graph embedding with restarts. In *Proceedings of the ACM Web*  
657 *Conference 2023*, pp. 478–488, 2023c.

658 Hongkuan Zhou, Da Zheng, Israt Nisa, Vasileios Ioannidis, Xiang Song, and George Karypis. Tgl: A  
659 general framework for temporal gnn training on billion-scale graphs. *Proceedings of the VLDB*  
660 *Endowment*, 15(8):1572–1580, 2022.

661 Yun Zhu, Jianhao Guo, and Siliang Tang. Sgl-pt: A strong graph learner with graph prompt tuning.  
662 *arXiv preprint arXiv:2302.12449*, 2023.

663

664

665

666

667

668

669

670

671

672

673

674

675

676

677

678

679

680

681

682

683

684

685

686

687

688

689

690

691

692

693

694

695

696

697

698

699

700

701

702 A TEMPORAL GAP AND SEMANTIC GAP  
703704 A.1 DEFINITION AND EXAMPLES OF THE GAPS  
705

706 **Temporal gap:** The gap caused by the time difference between training and inference data. For  
707 example, in TIG models, data (interaction edges) is input into the model chronologically, with training  
708 data occurring earlier than the data encountered during inference phase. During inference, the model  
709 trained on the training data is used to generate node representations. Previous TIG models usually rely  
710 on a memory module to store historical information. Specifically, they predict nodes’ future behaviors  
711 based on the stored memory, which is continuously updated. However, although the updating branch  
712 for temporal embedding modules generates new representations, the branch for memory updating  
713 often neglects this new information, leading to stale memory (Zhang et al., 2023c; Chen et al., 2023b).  
714 As a result, when there is a significant time gap between the training and inference data, the memory  
715 generated during inference cannot provide expressive historical information. Consequently, the  
716 training process becomes outdated with temporal interactions, resulting in ineffective predictions for  
717 future events (Zhang et al., 2023c).

718 **Semantic gap:** The gap between edge-level pretext task and node-level downstream task. For  
719 example, in the pre-training phase, the pretext task is typically link prediction, which usually brings  
720 connected nodes closer in the latent representation space. However, for node-level downstream tasks,  
721 such as node classification, using the node representations generated by the pre-trained model requires  
722 training an additional classification predictor. Since this process cannot access the pre-trained model,  
723 the output representations from the edge-level pre-trained model may lead to negative transfer when  
724 connected nodes have different labels, potentially resulting in misclassification of node labels (Sun  
725 et al., 2023). Intuitively, this is because edge-level pre-training strategy tends to enforce smoothness  
726 of node representations along observed edges, but there are many cases that two connected nodes  
727 have totally different labels, thereby exacerbating negative transfer (Sun et al., 2023).  
728

729 A.2 QUANTIFICATION OF THE GAPS  
730

731 Since these gaps are often implicitly embedded in node embeddings or representations, our idea  
732 is to assess them or identify the gaps through performance on downstream tasks. For example,  
733 using prompts that incorporate temporal information (Transformer or Projection TProG) reduces  
734 the temporal gap (i.e., in link prediction tasks, the models with these two TProGs outperform the  
735 baseline), while using only the Vanilla TProG without temporal information directly narrows the  
736 semantic gap (i.e., in node classification tasks, the models with Vanilla TProG successfully outperform  
737 the baseline). We propose a set of intuitive experiments to illustrate our claims.

738 **Temporal gap:** Building on the previous main experiments, we further split the inference (test) data  
739 into two parts, where the edge timestamps are increasing—i.e., interactions in the first part (1<sup>st</sup> Part,  
740 corresponds to “temporally proximal inference data” in Fig. 1 (a)) occur earlier and are closer to the  
741 training data than those in the second part (2<sup>nd</sup> Part, corresponds to “temporally distant inference data”  
742 in Fig. 1 (a)). We then apply them and conduct inference separately. If our hypothesis about the  
743 temporal gap holds true, the performance on the first part should be better than on the second part  
744 when using the baseline methods. When applying our proposed Transformer or Projection TProGs  
745 (we use Projection TProG and take MOOC dataset as example here for illustration), the performance  
746 should be improved, and the difference between the two parts should narrow. In line with main  
747 experiments, we use AP as the evaluation metric. As shown in the Tab. 3, the results align with our  
748 hypothesis. This validates the existence of the temporal gap and demonstrates that our method helps  
749 reduce it.

750 **Semantic gap:** Since the link prediction and node classification tasks both use the node embeddings  
751 generated by the pre-trained models for downstream tasks, a simple way to locate the semantic  
752 gap is to compare the same metric on both link prediction task and node classification task. For a  
753 fair comparison, we use AUROC as the evaluation metric for both tasks and conduct experiments  
754 on different dataset and backbone model combinations. By comparing the difference in AUROC  
755 between the two tasks before and after applying our proposed Vanilla TProG, it can be seen (from the  
Tab. 4) that the differences are narrowed after applying our “pre-train, prompt” training paradigm and  
TProG. This proves that the semantic gap indeed exists and that our method helps to narrow it.

756  
 757 Table 3: Quantification of Temporal Gap: Evaluated by AP (%). The 1<sup>st</sup> Part and the 2<sup>nd</sup> Part  
 758 corrspond to “temporally proximal inference data” and “temporally distant inference data” in Fig. 2  
 759 (c), respectively.

	Models	Baseline	Projection TProG	Gap Narrowed
Jodie	1 <sup>st</sup> Part	76.35	82.60	
	2 <sup>nd</sup> Part	72.38	80.17	38.73%
	GAP	3.98	2.44	
DyRep	1 <sup>st</sup> Part	74.81	82.71	
	2 <sup>nd</sup> Part	69.93	79.56	35.45%
	GAP	4.88	3.15	
TGN	1 <sup>st</sup> Part	88.34	88.91	
	2 <sup>nd</sup> Part	86.85	88.06	42.62%
	GAP	1.49	0.86	
TIGE	1 <sup>st</sup> Part	89.37	89.94	
	2 <sup>nd</sup> Part	88.01	89.10	38.24%
	GAP	1.36	0.84	
TIGER	1 <sup>st</sup> Part	87.16	89.56	
	2 <sup>nd</sup> Part	86.08	88.79	28.70%
	GAP	1.08	0.77	

774  
 775 Table 4: Quantification of Semantic Gap: Evaluated by AUROC (%). (Wiki. refers to Wikipedia  
 776 dataset)

	Dataset/Models	Baseline	Vanilla TProG	Gap Narrowed
Wiki/ TGN	Link Prediction	98.11	96.25	
	Node Classification	84.93	85.79	20.63%
	GAP	13.18	10.46	
Reddit/ Jodie	Link Prediction	97.91	97.57	
	Node Classification	58.48	69.22	28.10%
	GAP	39.43	28.35	
MOOC/ TIGER	Link Prediction	89.39	90.88	
	Node Classification	64.91	68.68	9.31%
	GAP	24.48	22.20	

### 789 A.3 HOW TPROGS NARROW THE GAPS

790  
 791 We now provide a brief theoretical analysis of how each TProG variant contributes to narrowing the  
 792 semantic and temporal gaps.

793 **Vanilla TProG** introduces node-specific prompt vectors that are directly optimized via node-level  
 794 supervision signals. This establishes a task-conditioned prompt generating, allowing the model to  
 795 re-contextualize outputted representations from frozen backbone toward the target task objective  
 796 (e.g., node classification), even without additional temporal signals. The effectiveness of such a setup  
 797 for node classification task confirms that semantic mismatch between edge-level pre-training and  
 798 node-level prediction can be mitigated through lightweight, learnable prompts.

799 **Projection TProG** builds upon Vanilla TProG by introducing explicit time conditioning, effectively  
 800 providing a soft temporal hint to the node representation. By projecting node-specific prompt vectors  
 801 into a temporal latent space using most recent interaction, it encourages the model to align the node  
 802 embedding from frozen backbone models with its current or recent temporal context. Intuitively, this  
 803 allows the prompt to act as a “reminder” or “hint” of recent temporal activity, helping the model  
 804 adapt representations to evolving dynamics. This partially compensates for the temporal mismatch  
 805 introduced during pre-training and enables better adaptation under time-varying behaviors. This  
 806 design enables downstream adaptation that is both semantically aligned and temporally consistent,  
 807 effectively narrowing the temporal gap and semantic gap that arise from stale backbone parameters.

808 **Transformer TProG** further generalizes this mechanism by conditioning prompt generation on  
 809 a sequence of recent interactions through self-attention. The prompt depends on the temporal  
 810 distribution and relational dynamics of recent neighbors. This captures higher-order temporal

810 dependencies and behavioral recency, which are crucial in interaction-dense data. As a result, the  
 811 prompt embedding space adapts in a temporally fine-grained manner.  
 812

813 In sum, the three variants form a progressive design spectrum: from task conditioning (Vanilla), to  
 814 timestamp-aware alignment (Projection), to dynamically evolving temporal modeling (Transformer).  
 815 This theoretically grounded progression supports our claim that the proposed prompting framework  
 816 can systematically mitigate both semantic and temporal gaps in TIG models.  
 817

## 818 B RELATED WORK 819

820 **Temporal Interaction Graph Models.** Temporal Interaction Graph representation learning models  
 821 (TIG models) are specifically designed to learn dynamic representations of the nodes in TIGs. These  
 822 models employ node representations to execute downstream tasks, including link prediction (by  
 823 computing node similarity) and node classification (through additional training of a classifier, i.e.,  
 824 projection head). The development of contemporary TIG models began with Jodie (Kumar et al.,  
 825 2019). Jodie utilizes two RNNs to dynamically update node representations and employs a projection  
 826 operator to estimate the embeddings of nodes that have not interacted for an extended period. DyRep  
 827 (Trivedi et al., 2019) introduces a deep temporal point process model, employing a dual-time scale  
 828 approach to effectively capture both association and communication dynamics. TGAT (Xu et al.,  
 829 2020) revolutionizes TIG models by incorporating an attention mechanism, wherein it substitutes  
 830 the original position coding with time coding to effectively aggregate information from a node’s  
 831 neighbors. Building on this, TGN (Rossi et al., 2020) introduces a memory module to store nodes’  
 832 historical interaction information, and integrating these developments into a cohesive framework.  
 833 TIGER (Zhang et al., 2023c) presents a model equipped with a dual-memory module, specifically  
 834 designed for enhanced aggregation of neighbor information. TIGER also introduces a restarter  
 835 module, responsible for generating surrogate representations, which serve as a warm initialization for  
 836 node representations. Additionally, several works are devoted to addressing challenges and resolving  
 837 specific complexities inherent in TIG models, including large-scale training (Zhou et al., 2022; Chen  
 838 et al., 2023b), noise dynamics (Zhang et al., 2023a), and node-wise long-term modeling (Zhang et al.,  
 839 2023b) issues. However, two critical issues persist: the limited adaptability of these models to new  
 840 data, and the semantic gap between pretext tasks and downstream tasks.

841 **Graph Prompt Learning.** Prompt-tuning methods, originating from the NLP domain (Devlin et al.,  
 842 2018; Liu et al., 2023a), have gained widespread use in adapting pre-trained language models to  
 843 a variety of downstream tasks. More recently, prompt learning has emerged in the graph domain  
 844 (Qin & Eisner, 2021; Tsimpoukelli et al., 2021; Sun et al., 2022; Zhu et al., 2023; Liu et al., 2023b;  
 845 Sun et al., 2023; Tan et al., 2023; Fang et al., 2023; Huang et al., 2023a; Shirkavand & Huang,  
 846 2023; Gong et al., 2023; Chen et al., 2023a; Ma et al., 2024; Ge et al., 2023; Yu et al., 2024a) as a  
 847 promising approach for directing downstream tasks. Pioneering works like GPPT (Sun et al., 2022)  
 848 focus on the node classification task, incorporating learnable prompts directly into graphs. Similarly,  
 849 GraphPrompt (Liu et al., 2023b) introduces a uniform prompt design, specifically tailored to address  
 850 both node- and graph-level downstream tasks. All-in-One (Sun et al., 2023) expands graph prompt  
 851 learning further by encompassing prompt tokens, structures, and insertion patterns, introducing a  
 852 comprehensive, albeit complex, prompting framework. Recent advancements in prompt learning  
 853 for static graphs have explored more fine-grained aspects of representation learning. GraphPrompt+  
 854 (Yu et al., 2024b) incorporates subgraph similarity and fixed structural patterns into the prompt  
 855 learning framework, enabling more structured guidance. ProNoG (Yu et al., 2024c) addresses the  
 856 challenges of non-homophilic graphs by focusing on structural irregularities and designing node-  
 857 specific prompting strategies. STGP (Hu et al., 2024) extends prompt learning to spatio-temporal  
 858 graphs in urban computing, highlighting cross-domain and multi-task transfer through a two-stage  
 859 prompting mechanism. Nevertheless, there is a noticeable absence of prompt tuning methods  
 860 specifically designed for the temporal interaction graphs, as existing static graph prompting works  
 861 lack a temporal consideration and exhibit weak expressiveness.

862 **Comparison with Contemporaneous Work.** We identify a contemporaneous work, DyGPrompt (Yu  
 863 et al., 2025), and provide a conceptual comparison as follows. While both TIGPrompt and DyGPrompt  
 864 aim to bridge the gap between pre-training and downstream tasks in dynamic graph learning through  
 865 prompt-based adaptation, the two methods differ in design goals and technical implementation.  
 866 DyGPrompt introduces a dual-prompt and dual-conditioning framework, utilizing both feature and

864 temporal prompts along with a node-time co-conditioning mechanism. This design enables fine-  
 865 grained joint modeling of node features and timestamps through a sophisticated co-conditioning  
 866 process. In contrast, our work identifies two fundamental gaps—temporal and semantic—in traditional  
 867 TIG training paradigms, and proposes a novel prompt-based training approach to bridge them.  
 868 Specifically, we propose to use “pre-train, prompt” paradigm or “pre-train, prompt-based fine-tune”  
 869 paradigm, bridging the temporal and semantic gaps and introduce TProGs to construct prompts that  
 870 incorporate temporal information, aligning with the inherent characteristics of TIGs. Our approach  
 871 emphasizes a new training paradigm for TIGs and lightweight, time-aware prompt generation through  
 872 variants of TProGs. We thus consider DyGPrompt a complementary contemporaneous work. While  
 873 DyGPrompt emphasizes fine-grained adaptivity in node-time modeling, TIGPrompt offers a simple,  
 874 efficient, and broadly applicable solution. Due to the unavailability of DyGPrompt’s source code, we  
 875 do not include a direct empirical comparison in our paper.  
 876

## C DATASETS

879 In alignment with previous studies (Kumar et al., 2019; Trivedi et al., 2019; Rossi et al., 2020; Zhang  
 880 et al., 2023c), we utilize four public datasets made available by the authors of Jodie (Kumar et al.,  
 881 2019). Detailed statistics of these datasets can be found in Tab. 5.

882 Table 5: Dataset Statistics.  $d_n$  and  $d_e$  indicate the dim of nodes and edges, respectively.  
 883

	# Nodes	# Edges	$d_n$	$d_e$	Classes
Wikipedia	9,227	157,474	172	172	2
Reddit	10,984	672,447	172	172	2
MOOC	7,144	411,749	172	172	2
LastFM	1,980	1,293,103	172	172	-

## D EXPERIMENTS UNDER “PRE-TRAIN, PROMPT-BASED FINE-TUNE”

### D.1 LINK PREDICTION

894 We provide the complete experiment results for the “pre-train, prompt-based fine-tune” paradigm link  
 895 prediction task in both transductive and inductive settings in Tab. 6.  
 896

### D.2 NODE CLASSIFICATION

#### D.2.1 TRAINING STRATEGIES

901 Under the “pre-train, prompt-based fine-tune” paradigm for the node classification task, three different  
 902 strategies can be applied: (1) directly employing the TProG trained in the link prediction task to  
 903 generate prompts; (2) using the link prediction-trained TProG to initialize a TProG and then further  
 904 optimizing it during node classification; and (3) discarding the previously TProG and re-initializing  
 905 a new one for optimization alongside the node classification task.

906 We choose the first strategy for our experiments, with the outcomes detailed in Tab. 7. Notably, a part  
 907 of these results exceed those achieved under the “pre-train, prompt” paradigm. However, similar to  
 908 the link prediction task, this approach demands additional training resources. A comparison of three  
 909 training strategies is presented in Appendix D.2.2. This comparison demonstrates that applying the  
 910 other two strategies has the potential to improve the performance of node classification tasks.  
 911

#### D.2.2 COMPARISON BETWEEN THREE STRATEGIES OF NODE CLASSIFICATION TRAINING

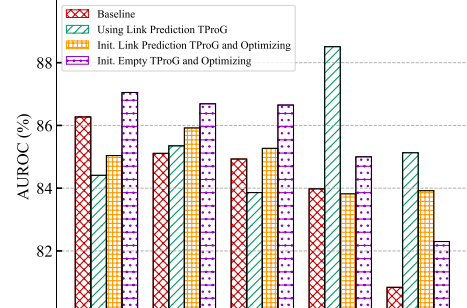
913 Beyond the initial experiments conducted under “pre-train, prompt-based fine-tune” for the node  
 914 classification task, we extend our investigation to include various training strategies outlined in  
 915 Appendix D.2.1. A series of experiments was conducted using the Wikipedia dataset, employing the  
 916 Projection TProG. The outcomes of these experiments are illustrated in Fig. 6. The results indicate  
 917 that our method outperforms the baseline models when different strategies are applied, thereby  
 demonstrating the effectiveness of our approach.

918  
919  
920  
Table 6: Full results of Average Precision (%) for the link prediction tasks under the “pre-train,  
prompt-based fine-tune” paradigm in both Transductive and Inductive settings.

Transductive Link Prediction									Inductive Link Prediction			
TProG		Wiki	Reddit	MOOC	LastFM	Wiki	Reddit	MOOC	LastFM			
Jodie	Baseline	94.62 $\pm$ 0.5	97.11 $\pm$ 0.3	76.50 $\pm$ 1.8	68.77 $\pm$ 3.0	93.11 $\pm$ 0.4	94.36 $\pm$ 1.1	77.83 $\pm$ 2.1	82.55 $\pm$ 1.9			
	Vanilla	94.22 $\pm$ 0.9	97.17 $\pm$ 0.3	76.32 $\pm$ 1.6	74.45 $\pm$ 1.3	92.66 $\pm$ 1.0	93.91 $\pm$ 0.9	74.58 $\pm$ 2.5	81.27 $\pm$ 1.0			
	Transformer	97.01 $\pm$ 0.4	98.25 $\pm$ 0.1	85.52 $\pm$ 0.6	76.48 $\pm$ 1.5	96.13 $\pm$ 0.5	96.71 $\pm$ 0.3	84.33 $\pm$ 0.6	84.63 $\pm$ 1.3			
	Projection	96.72 $\pm$ 0.6	98.84 $\pm$ 0.1	83.03 $\pm$ 0.3	88.82 $\pm$ 0.5	95.36 $\pm$ 0.6	97.79 $\pm$ 0.2	81.72 $\pm$ 1.3	92.51 $\pm$ 0.4			
DyRep	Baseline	94.59 $\pm$ 0.2	97.98 $\pm$ 0.1	75.37 $\pm$ 1.7	68.77 $\pm$ 2.1	92.05 $\pm$ 0.3	95.68 $\pm$ 0.2	78.55 $\pm$ 1.1	81.33 $\pm$ 2.1			
	Vanilla	90.48 $\pm$ 1.1	97.15 $\pm$ 0.2	74.88 $\pm$ 2.5	72.96 $\pm$ 0.5	88.50 $\pm$ 1.3	93.31 $\pm$ 0.7	73.42 $\pm$ 2.7	80.79 $\pm$ 1.8			
	Transformer	95.62 $\pm$ 0.4	98.17 $\pm$ 0.1	84.81 $\pm$ 1.1	74.22 $\pm$ 1.8	94.52 $\pm$ 0.6	96.61 $\pm$ 0.2	83.38 $\pm$ 0.7	83.74 $\pm$ 2.5			
	Projection	97.19 $\pm$ 0.2	98.96 $\pm$ 0.1	82.53 $\pm$ 1.7	88.83 $\pm$ 0.4	96.11 $\pm$ 0.3	97.78 $\pm$ 0.2	81.51 $\pm$ 1.0	92.59 $\pm$ 0.4			
TGN	Baseline	98.46 $\pm$ 0.1	98.70 $\pm$ 0.1	85.88 $\pm$ 3.0	71.76 $\pm$ 5.3	97.81 $\pm$ 0.1	97.55 $\pm$ 0.1	85.55 $\pm$ 2.9	80.42 $\pm$ 4.9			
	Vanilla	97.72 $\pm$ 0.2	98.32 $\pm$ 0.1	88.58 $\pm$ 1.1	72.69 $\pm$ 5.0	96.94 $\pm$ 0.1	96.51 $\pm$ 0.3	87.89 $\pm$ 0.9	78.97 $\pm$ 3.9			
	Transformer	98.25 $\pm$ 0.1	98.68 $\pm$ 0.1	89.95 $\pm$ 1.7	77.79 $\pm$ 3.2	97.59 $\pm$ 0.2	97.62 $\pm$ 0.1	89.11 $\pm$ 1.2	83.48 $\pm$ 2.4			
	Projection	98.38 $\pm$ 0.1	99.29 $\pm$ 0.0	90.00 $\pm$ 1.4	90.08 $\pm$ 0.9	97.81 $\pm$ 0.1	98.61 $\pm$ 0.1	89.15 $\pm$ 1.6	92.64 $\pm$ 0.9			
TIGE	Baseline	98.83 $\pm$ 0.1	99.04 $\pm$ 0.0	89.64 $\pm$ 0.9	87.85 $\pm$ 0.9	98.45 $\pm$ 0.1	98.39 $\pm$ 0.1	89.51 $\pm$ 0.7	90.14 $\pm$ 1.0			
	Vanilla	98.84 $\pm$ 0.0	98.87 $\pm$ 0.0	90.18 $\pm$ 0.7	89.06 $\pm$ 0.5	98.37 $\pm$ 0.0	97.82 $\pm$ 0.2	89.59 $\pm$ 0.5	91.06 $\pm$ 0.4			
	Transformer	98.99 $\pm$ 0.0	99.20 $\pm$ 0.0	92.14 $\pm$ 0.9	91.22 $\pm$ 0.3	98.58 $\pm$ 0.0	98.70 $\pm$ 0.1	91.22 $\pm$ 0.8	92.81 $\pm$ 0.3			
	Projection	99.12 $\pm$ 0.0	99.48 $\pm$ 0.0	91.68 $\pm$ 0.4	95.30 $\pm$ 0.1	98.84 $\pm$ 0.0	99.16 $\pm$ 0.0	91.16 $\pm$ 0.4	96.20 $\pm$ 0.1			
TIGER	Baseline	98.90 $\pm$ 0.0	99.02 $\pm$ 0.0	86.99 $\pm$ 1.6	85.17 $\pm$ 0.2	98.58 $\pm$ 0.0	98.59 $\pm$ 0.0	86.42 $\pm$ 1.7	89.11 $\pm$ 0.3			
	Vanilla	98.90 $\pm$ 0.0	98.84 $\pm$ 0.0	85.12 $\pm$ 1.1	85.59 $\pm$ 0.5	98.49 $\pm$ 0.1	98.13 $\pm$ 0.1	84.37 $\pm$ 0.8	88.43 $\pm$ 0.6			
	Transformer	99.05 $\pm$ 0.0	99.18 $\pm$ 0.0	87.00 $\pm$ 0.9	87.84 $\pm$ 0.2	98.68 $\pm$ 0.0	98.78 $\pm$ 0.0	86.07 $\pm$ 1.0	90.50 $\pm$ 0.3			
	Projection	99.17 $\pm$ 0.0	99.49 $\pm$ 0.0	87.83 $\pm$ 0.6	93.50 $\pm$ 0.2	98.88 $\pm$ 0.0	99.28 $\pm$ 0.0	87.38 $\pm$ 0.9	94.90 $\pm$ 0.3			
GraphMiner	Baseline	97.25 $\pm$ 0.0	97.31 $\pm$ 0.0	82.78 $\pm$ 0.2	75.61 $\pm$ 0.2	96.65 $\pm$ 0.0	95.26 $\pm$ 0.0	81.41 $\pm$ 0.2	82.11 $\pm$ 0.4			
	Vanilla	96.24 $\pm$ 0.1	97.52 $\pm$ 0.0	81.27 $\pm$ 0.3	76.91 $\pm$ 0.3	95.65 $\pm$ 0.1	94.25 $\pm$ 0.2	79.27 $\pm$ 0.9	81.86 $\pm$ 0.4			
	Transformer	97.45 $\pm$ 0.0	98.12 $\pm$ 0.0	84.09 $\pm$ 0.9	78.19 $\pm$ 0.3	97.02 $\pm$ 0.0	96.40 $\pm$ 0.0	81.61 $\pm$ 1.2	83.81 $\pm$ 0.3			
	Projection	98.99 $\pm$ 0.2	99.23 $\pm$ 0.0	87.48 $\pm$ 0.2	88.84 $\pm$ 3.1	97.78 $\pm$ 0.5	94.43 $\pm$ 0.9	84.76 $\pm$ 0.1	86.92 $\pm$ 2.3			
DyGFormer	Baseline	99.03 $\pm$ 0.0	99.22 $\pm$ 0.0	87.52 $\pm$ 0.5	93.00 $\pm$ 0.1	98.59 $\pm$ 0.0	98.84 $\pm$ 0.0	86.96 $\pm$ 0.4	94.23 $\pm$ 0.1			
	Vanilla	98.97 $\pm$ 0.0	99.16 $\pm$ 0.0	86.42 $\pm$ 0.4	92.78 $\pm$ 0.1	98.55 $\pm$ 0.0	98.78 $\pm$ 0.0	85.67 $\pm$ 0.5	94.14 $\pm$ 0.0			
	Transformer	99.07 $\pm$ 0.1	99.50 $\pm$ 0.1	87.92 $\pm$ 0.3	93.76 $\pm$ 0.1	98.76 $\pm$ 0.1	99.12 $\pm$ 0.1	87.17 $\pm$ 0.3	94.69 $\pm$ 0.3			
	Projection	99.84 $\pm$ 0.0	99.87 $\pm$ 0.0	91.06 $\pm$ 0.3	95.12 $\pm$ 0.2	99.44 $\pm$ 0.0	98.79 $\pm$ 0.2	89.08 $\pm$ 0.2	94.99 $\pm$ 0.4			

948  
949  
950  
951  
Table 7: AUROC (%) for dynamic node clas-  
sification task under “pre-train, prompt-based  
fine-tune”.

Node Classification								
TProG		Wiki	Reddit	MOOC				
Jodie	Baseline	86.27 $\pm$ 2.2	58.48 $\pm$ 2.6	65.39 $\pm$ 1.1				
	Vanilla	84.82 $\pm$ 0.3	63.87 $\pm$ 1.4	66.32 $\pm$ 1.8				
	Transformer	86.42 $\pm$ 2.4	67.19 $\pm$ 1.0	71.36 $\pm$ 0.8				
	Projection	84.41 $\pm$ 3.0	62.27 $\pm$ 3.8	75.89 $\pm$ 1.5				
DyRep	Baseline	85.11 $\pm$ 1.4	62.77 $\pm$ 2.1	66.68 $\pm$ 3.4				
	Vanilla	88.64 $\pm$ 1.8	58.64 $\pm$ 2.7	65.00 $\pm$ 2.2				
	Transformer	83.73 $\pm$ 0.3	64.58 $\pm$ 2.2	71.98 $\pm$ 2.8				
	Projection	85.35 $\pm$ 0.5	58.84 $\pm$ 2.1	75.09 $\pm$ 1.3				
TGN	Baseline	84.93 $\pm$ 1.1	65.99 $\pm$ 3.8	69.80 $\pm$ 1.8				
	Vanilla	82.49 $\pm$ 2.7	62.93 $\pm$ 3.8	64.66 $\pm$ 3.9				
	Transformer	82.43 $\pm$ 1.1	64.67 $\pm$ 3.5	70.03 $\pm$ 2.9				
	Projection	83.86 $\pm$ 1.4	60.28 $\pm$ 4.8	77.15 $\pm$ 3.1				
TIGE	Baseline	83.98 $\pm$ 3.4	65.36 $\pm$ 2.9	69.61 $\pm$ 2.5				
	Vanilla	81.43 $\pm$ 6.8	62.46 $\pm$ 2.5	70.35 $\pm$ 0.8				
	Transformer	85.87 $\pm$ 2.0	64.14 $\pm$ 1.6	67.61 $\pm$ 5.9				
	Projection	88.51 $\pm$ 0.8	59.08 $\pm$ 3.9	78.04 $\pm$ 3.2				
TIGER	Baseline	80.84 $\pm$ 4.6	62.58 $\pm$ 1.3	64.91 $\pm$ 5.2				
	Vanilla	84.93 $\pm$ 2.5	64.22 $\pm$ 1.8	68.16 $\pm$ 2.9				
	Transformer	83.95 $\pm$ 4.4	60.75 $\pm$ 1.3	68.26 $\pm$ 1.8				
	Projection	85.13 $\pm$ 1.4	61.20 $\pm$ 2.2	81.58 $\pm$ 1.2				

952  
953  
954  
955  
956  
957  
958  
959  
960  
961  
962  
963  
964  
965  
966  
967  
968  
969  
970  
971  
Figure 6: Comparison between three different “pre-train, prompt-based fine-tune” node classification training strategies (Wikipedia dataset, employing the Projection TProG).

## E CONTINUED EXPERIMENT RESULTS

## E.1 RESULTS FOR LIMITED PROMPT DATA EXPERIMENTS

972  
973  
974  
975  
976  
977  
978  
979  
980  
981  
We provide the complete experiment results for limited prompt data analysis in Fig. 7).

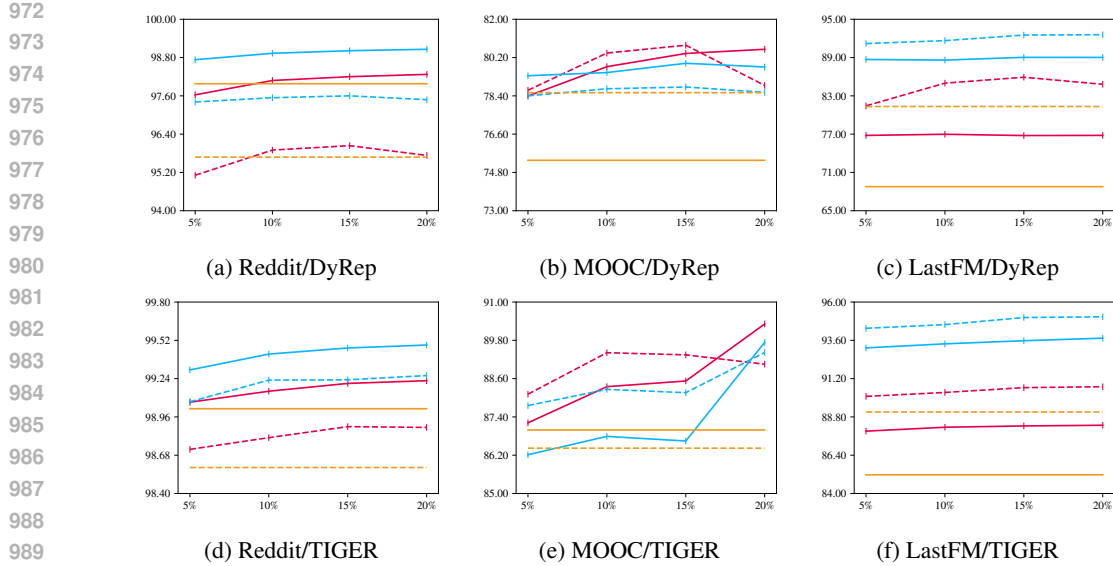


Figure 7: Performance w.r.t the Proportion of Prompting Data. This is a continued figure of Fig. 5.

## E.2 APPLYING TO NON-MEMORY-BASED TIG METHODS

The basic baseline models utilized in this paper are based on the TGN architecture (Rossi et al., 2020), which employ a memory module to store historical interaction information for nodes. Recently, various model architectures have been proposed by researchers, incorporating different backbone models. GraphMixer (Cong et al., 2023) and DyGFormer (Yu et al., 2023) are two representative works based on MLP and Transformer architectures, respectively. Although GraphMixer and DyGFormer do not share a similar architecture with the memory-based TIG methods (i.e., methods based on TGN architecture or TGN-based methods), they similarly utilize representations for downstream tasks. Our proposed TIGPrompt, wherein the prompt is fused with node representations for use in downstream tasks, is thus thought to potentially combine effectively with GraphMixer and DyGFormer. To explore this possibility, we conduct a set of experiments based on these two models. As demonstrated in Tab. 1, 2 and 6, our proposed TIGPrompt can effectively enhance the performance of non-memory-based TIG models on both link prediction and node classification tasks.<sup>2</sup>

Although we only implement experiments on GraphMixer and DyGFormer, the underlying mechanism is similar for other methods that build upon them, such as DyGMamba (Ding et al., 2024) and FreeDyG (Tian et al., 2024). Our proposed method is not a new backbone model, but rather a general training paradigm designed to adapt existing TIG models to downstream tasks in a more flexible and efficient manner. While the motivation is inspired by TGN-based architectures, our empirical evaluation covers models beyond memory-based designs, i.e., GraphMixer (MLP-based) and DyGFormer (Transformer-based). These results demonstrate that TIGPrompt is broadly compatible with different backbone types, as long as they follow the traditional “pre-train, predict” training paradigm.

## F TPROG VARIANT SELECTION

We provide guidance on selecting among the three TProG variants according to dataset characteristics and computational–performance considerations.

Vanilla TProG, with its lightweight  $\mathcal{O}(|\mathcal{V}|)$  node-dependent parameters, focuses primarily on mitigating the semantic gap and offers the fastest inference among all variants. It is well suited for datasets with relatively few nodes, scenarios requiring low-latency inference, and node classification tasks where semantic alignment dominates over temporal dynamics.

<sup>2</sup>Experiments are conducted based on the open-source repository [DyGLib](#) (Yu et al., 2023). We employ the best model configurations as provided by DyGLib for the pre-training process with default settings.

1026 Projection TProG also scales with  $\mathcal{O}(|\mathcal{V}|)$  parameters but incorporates temporal cues, enabling it to  
 1027 address both the semantic and temporal gaps while maintaining high computational efficiency. This  
 1028 variant is particularly appropriate for small- to medium-scale datasets or applications that require a  
 1029 balanced trade-off between temporal expressiveness and inference cost.

1030 In contrast, Transformer TProG employs a lightweight Transformer encoder with parameters scaling  
 1031 as  $\mathcal{O}(d)$ , making it more scalable for large graphs and especially effective when modeling complex or  
 1032 irregular temporal patterns. It typically achieves the strongest performance in settings where temporal  
 1033 gap mitigation is crucial and accuracy is prioritized over inference speed.  
 1034

## 1035 G DATA AMOUNT FOR TRAINING

1036 In this section, we analyze the amount of data used in our experiment for training and the reasons  
 1037 behind the resulting experimental outcomes. Note that all experiments use 15% of the data for  
 1038 validation and a different 15% for testing. The data amount used for training is summarized in Tab. 8.  
 1039

1040 Firstly, we use 50% of the data for pre-training, followed by 20% of the data for prompt tuning,  
 1041 making a total of 70% of the data used for training (Sec. 4.3 and 4.4). This setup is to align with the  
 1042 70% data for training of baseline models. Additionally, we adjust the amount of 20% prompt tuning  
 1043 data through comparative experiments to explore the effects of different tuning data volumes (Sec.  
 1044 4.7.2). Then, we compare the situation where only a small amount of training data is available, i.e.,  
 1045 the baseline uses only 20% of the data for training, whereas our method uses only 10% of the data for  
 1046 pre-training and 10% for prompt tuning, making a total of 20% of the data for overall training (Sec.  
 1047 4.7.1).  
 1048

1049 It is natural that some experimental results may show degradation when only 10% of the data is  
 1050 allocated for pre-training, compared to the baseline results achieved with 70% of the data used for  
 1051 training. This can be attributed to the substantial decrease in the amount of overall training data.  
 1052 However, as can be seen from Tab. 2, almost all results of our method surpass the baseline of using  
 1053 only 20% of the data for training, with part of results (marked in blue in the Tab. 2) surpass the  
 1054 baseline models training with 70% of data. This demonstrates the effectiveness of our proposed  
 1055 method.

1056 Table 8: Training Data Amount for different experiments.  
 1057

1058 Experiments	1059 Methods	1060 Pre-train/ Training	1061 Prompt tuning	1062 Total for Training
1060 Main (Sec. 4.3 and 4.4)	1061 Baseline TIGPrompt	1062 70% 50%	1063 / 20%	1064 70% 70%
1063 Limited Training Data (Sec. 4.7.1)	1064 Baseline TIGPrompt	1065 20% 10%	1066 / 10%	1067 20% 20%
1067 Limited Prompt Data (Sec. 4.7.2)	1068 Baseline TIGPrompt	1069 70% 50%	1070 / 5%-20%	1071 70% 55%-70%

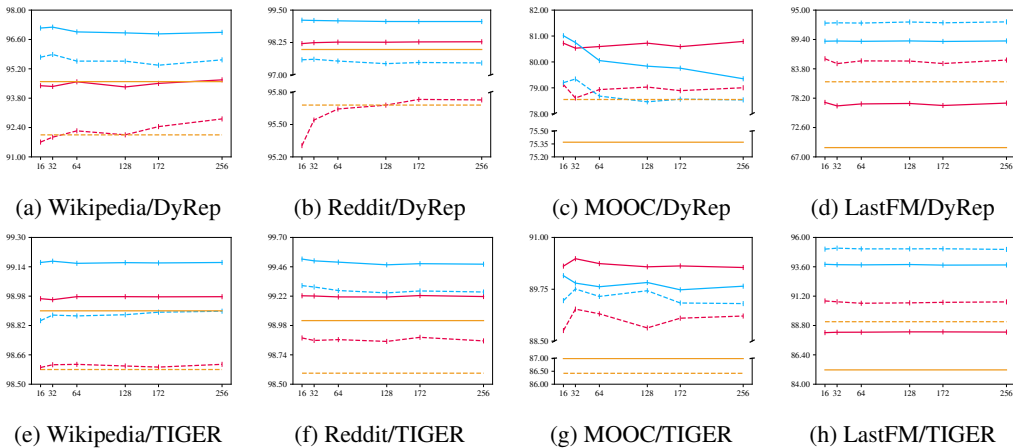
1068 **Discussions on “Weak Supervision”.** In the original prompt learning literature from NLP (Devlin  
 1069 et al., 2018; Liu et al., 2023a), the concept of few-shot learning is well-established. However, this  
 1070 notion is difficult to directly translate into the context of TIGs. In TIGs, a few-shot setting can only  
 1071 be simulated by restricting the amount of data used during either the fine-tuning phases. Notably,  
 1072 temporal link prediction—the core task for both pretext and downstream objectives in many TIG  
 1073 models—does not lend itself easily to a few-shot formulation. This is because the supervision signal  
 1074 arises from future interactions rather than class labels, making it hard to define a fixed number of  
 1075 “support” instances typical of few-shot learning. For node classification, existing few-shot methods  
 1076 designed for NLP (Devlin et al., 2018; Liu et al., 2023a) or static graphs (Liu et al., 2023b; Sun  
 1077 et al., 2023) are also not directly applicable. In TIGs, the task typically involves dynamic node  
 1078 classification, where the label of a node may evolve over time. Additionally, training a classification  
 1079 head in this setting still requires a minimum amount of data, further complicating the establishment  
 of a rigorous few-shot regime. As such, we argue that constructing an effective few-shot setting for  
 TIG representation learning remains an open and under-explored challenge.

1080 To address this, we introduce the concept of weak supervision in TIG prompt learning. Here, weak  
 1081 supervision refers to training under limited data availability—not only during prompt tuning but also  
 1082 throughout the entire training pipeline, including pre-training.

1083 Specifically, we explore scenarios where only 5%–20% of the data is used for prompt tuning (with  
 1084 a total training budget of 55%–70% data, please refer to Sec.4.7.1), or even more extreme cases  
 1085 where 10% is allocated for pre-training and another 10% for prompt tuning—resulting in a total  
 1086 training budget of just 20% data (please refer to Sec.4.7.2). These settings demonstrate the strong data  
 1087 efficiency and weak-supervision tolerant of our method, particularly when compared to traditional  
 1088 baselines trained on the full 70% of the data, which still underperformed.

## 1090 H PARAMETER ANALYSIS

1091 In these experiments, we explore the impacts of the dimension of the prompt vector. Additionally, we  
 1092 examine whether increasing the dimensions could yield even better results. As shown in Fig. 8, the  
 1093 results indicate that a 64-dimensional prompt vector suffices to surpass the baseline performance in  
 1094 most cases. While higher dimensions do improve outcomes, they also increase the model’s complexity.  
 1095 Researchers, therefore, should weigh the trade-off between experimental effectiveness and resource  
 1096 efficiency when selecting the optimal prompt vector dimension.



1114 Figure 8: Performance w.r.t the Prompts Dimension. This figure shares the same legend with Fig. 5.  
 1115

## 1116 I EFFICIENCY ANALYSIS

1117 We first record the training time on the Nvidia V100 GPU of the most commonly used baseline model,  
 1118 TGN (Rossi et al., 2020), on two datasets. As shown in Tab. 9, the Transformer TProG exhibits  
 1119 modest time efficiency due to the inherent computational slowness of transformers. However, the  
 1120 other two TProGs both register substantial efficiency enhancements. The results demonstrate that the  
 1121 proposed method is indeed lightweight.

1122 We further provide a theoretical comparison between TProGs and TGN (other backbones exhibit  
 1123 similar complexity).

1124 For TGN, assuming the node embeddings, including the memory, and prompts use the same dimension  
 1125  $d_n$  as the input node features, and edge features dimension is  $d_e$ .

1126 The complexity for the time encoding is  $\mathcal{O}(d_{te})$ , where  $d_{te}$  is the dimension of time encoding. The  
 1127 memory module’s complexity is  $\mathcal{O}(|\mathcal{V}| \cdot d_n)$ , where  $|\mathcal{V}|$  is the total number of nodes. TGN employs  
 1128 a GRU as the memory updater, which has a complexity of  $\mathcal{O}((d_{te} + 2d_n + d_e) \cdot d_n + d_n^2)$ . TGN  
 1129 uses multi-head attention to compute node embeddings, with the complexity of  $\mathcal{O}(L \cdot ((d_n + d_e +  
 1130 d_{te}) \cdot h + (n + 1)^2 + h \cdot d_n))$ , where  $h$  is hidden layer dimension,  $L$  is number of layers, and  $n$  is  
 1131 the number of neighbors. Thus, the overall space complexity of TGN can be expressed as adding  
 1132 the complexity of the time encoding, memory module, and the multi-head attention module.  
 1133

1134 these four terms together. As observed, the memory module contributes significantly to TGN’s space  
 1135 complexity, especially for large graphs.

1136 In contrast, Vanilla TProG introduces only a learnable prompt vector for each node. Its overall  
 1137 complexity is  $\mathcal{O}(|\mathcal{V}| \cdot d_n)$ . This results in a lower computational complexity compared to TGN.

1138 Transformer TProG employs a 1-layer Transformer to generate prompts, with a complexity of  
 1139  $\mathcal{O}((2d_n + 1 + d_e + d_{te}) \cdot h + K^2 + h \cdot d_n)$ , as derived in Equ. 2, where  $K$  is the sampled historical  
 1140 interactions used to compute the prompts. Notably, this complexity is independent of the number of  
 1141 nodes, i.e.,  $|\mathcal{V}|$ , making it more efficient for larger TIGs with many nodes.

1142 Projection TProG shares a similar structure with Vanilla TProG in maintaining a node-specific prompt  
 1143 vector, but further incorporates a lightweight MLP to model temporal dependencies. Its complexity  
 1144 can be expressed as  $\mathcal{O}(d_n \cdot d_{te} + d_n^2 + |\mathcal{V}| \cdot d_n)$ , which remains lower than that of TGN, while offering  
 1145 improved modeling capability.

1146 As the results in Tab. 9 and the complexity analysis show, our method boosts efficiency and lowers  
 1147 training resources versus the baselines. Despite its efficiency, our method still yields favorable  
 1148 outcomes in downstream tasks.

1151 Table 9: Training time for one epoch (in seconds) comparison.

	TProG	Training Time
Wikipedia	Baseline	15.1
	Vanilla	4.4(-70.9%)
	Transformer	14.4(-4.6%)
	Projection	4.2(-72.2%)
MOOC	Baseline	36.9
	Vanilla	12.6(-65.9%)
	Transformer	23.2(-37.1%)
	Projection	12.4(-66.4%)

## 1163 J IMPLEMENTATION DETAILS

1164 We implement our methods in PyTorch, building on the official implementations of TGN (Rossi et al.,  
 1165 2020), TIGER (Zhang et al., 2023c) and DyGFormer (Yu et al., 2023). Unless specified otherwise,  
 1166 we adhere to the default hyper-parameters listed in Tab. 10 and maintain the same data pre-processing  
 1167 and hyper-parameter settings as in the original implementations. Since we strictly follow the settings  
 1168 in the original implementations, we reuse the baseline results reported in (Zhang et al., 2023c) as  
 1169 baselines. To fairly assess the effect of our proposed training framework, we deliberately refrain  
 1170 from adjusting hyper-parameters, and treat negative sampling strategies (Yu et al., 2023; Huang et al.,  
 1171 2023b) as intrinsic, hyper-parameter-level choices specific to each backbone model (e.g., DyGFormer  
 1172 (Yu et al., 2023) adopts different strategies across datasets and model variants). Consequently, we keep  
 1173 all default configurations unchanged and integrate TIGPrompt on top of the original implementations.  
 1174 This ensures that the observed performance gains stem from the prompting paradigm rather than  
 1175 backbone-specific heuristics.

1176 All experiments are conducted on a single server with 72 cores, 32GB memory, and single Nvidia  
 1177 Tesla V100 GPU.

## 1181 K LIMITATIONS AND FUTURE WORK

1182 We provide a novel training paradigm for TIGs, while we may need to conduct a certain amount  
 1183 of additional experiments to test which TProG is more suitable for the current dataset/baseline  
 1184 combination for performance consideration. However, for the improvement in performance, we  
 1185 believe this extra effort is worthwhile. We also provide practical guidance for selecting among  
 1186 different TProG variants in Appendix F. Our paper has demonstrated that all three TProGs are  
 1187 effective through extensive experiments. The current work only focuses on and considers a series of

1188  
1189  
1190  
1191  
1192  
1193  
1194  
1195  
1196  
1197  
1198  
1199  
1200  
1201  
1202  
1203  
1204  
1205  
1206  
1207  
1208  
1209  
1210  
1211  
1212  
1213  
1214  
1215  
1216  
1217  
1218  
1219  
1220  
1221  
1222  
1223  
1224  
1225  
1226  
1227  
1228  
1229  
1230  
1231  
1232  
1233  
1234  
1235  
1236  
1237  
1238  
1239  
1240  
1241  
Table 10: Default values of hyper-parameters.

Hyper-parameter	Value
Batch size (Pre-training)	200
Batch size (Prompt tuning)	100
Learning rate	0.0001
Optimizer	Adam
Prompt dimension	172
Memory dimension	172
Negative sampling	Same as backbone models

baseline models based on TGN. The current method only considers individual datasets and does not account for integrating multiple datasets to construct a large dataset for pre-training.

In light of our study's scope and findings, we identify several potential directions for future work:

- Designing TProG variants to better match various baseline models and datasets.
- Utilizing larger datasets to complete comprehensive pre-training processes, followed by fine-tuning or prompt tuning for diverse datasets.
- Extending our methodologies to additional downstream tasks, including graph-level tasks.

## L THE USE OF LARGE LANGUAGE MODELS

The Large Language Models are only used for editing and formatting purposes.